Enabling Near-Field Communications: Beam Shaping, Optimization, and Channel/Data Estimation

Prof. Koji Ishibashi

Advanced Wireless & Communication Research Center (AWCC)
The University of Electro-Communications, Tokyo Japan

This work was supported by in part by the JST AdCORP under Grant JPMJKB2307.

May 16, 2025

The University of Electro-Communications

- Founded in 1918 as the Technical Institute for Wireless Communications.
- Became national university in 1949.
- The only national university in Japan without a place name.
- 304 faculty members, 136 staffs, 3371 undergrads, and 1,430 graduates.
- Notable faculty members
  - Te Sun Han & Kingo Kobayashi
  - Kunihiko Fukushima
- Notable almuni
  - Ken Kutaragi (Father of PlayStation)

国立大学法人
電気通信大学
The University of Electro-Communications

Introduction of Our Research Center

☐ Advanced Wireless & Communications Research Center (AWCC)

- Japan's only national university research center specializing in wireless communications
- 3 dedicated professors, 6 concurrent professors
- Leading many national research projects

☐ Consortium for Wireless Innovation and Research EXchange

- Founded in 2023
- A platform for "industry-academia collaboration"
- To build up a strong network of researchers in Japan
- 8 Sponsors, 68 Members from 14 Organizations

Main Contributors of This Talk

Sota Uchimura
(2nd-year doctoral student)

Kabuto Arai
(3rd-year doctoral student)

Prof. Josep M. Jornet
(Northeastern Univ.)

Hiroki Iimori, Ph.D.
(Ericsson Research Japan)

Paulo V. Klaine, Ph.D.
(Ericsson Research Japan)

Szabolcs Malomsoky, Ph.D.
(Ericsson Research Japan)

Need for Higher-Frequency Bands

- Leveraging higher-frequency bands is essential to further increase data rates.
  - **High directivity** is needed to compensate for severe path loss.

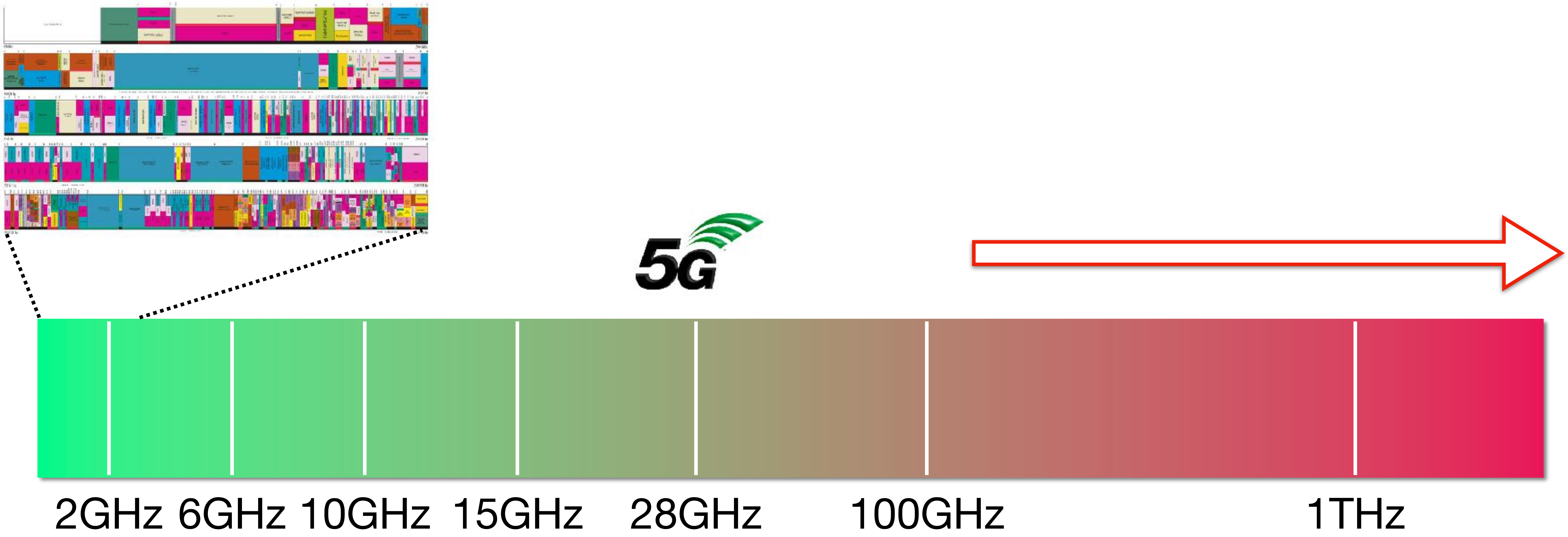

Channel Instability in High Frequency Bands

AWCC
Advanced Wireless and Communication Research Center

- ☐ High directivity → narrow beams
- ☐ High photon energy → strong reflection and/or absorption by materials
- ☐ Short wavelengths → significant diffraction even from small objects

Severe blockage losses by common objectives

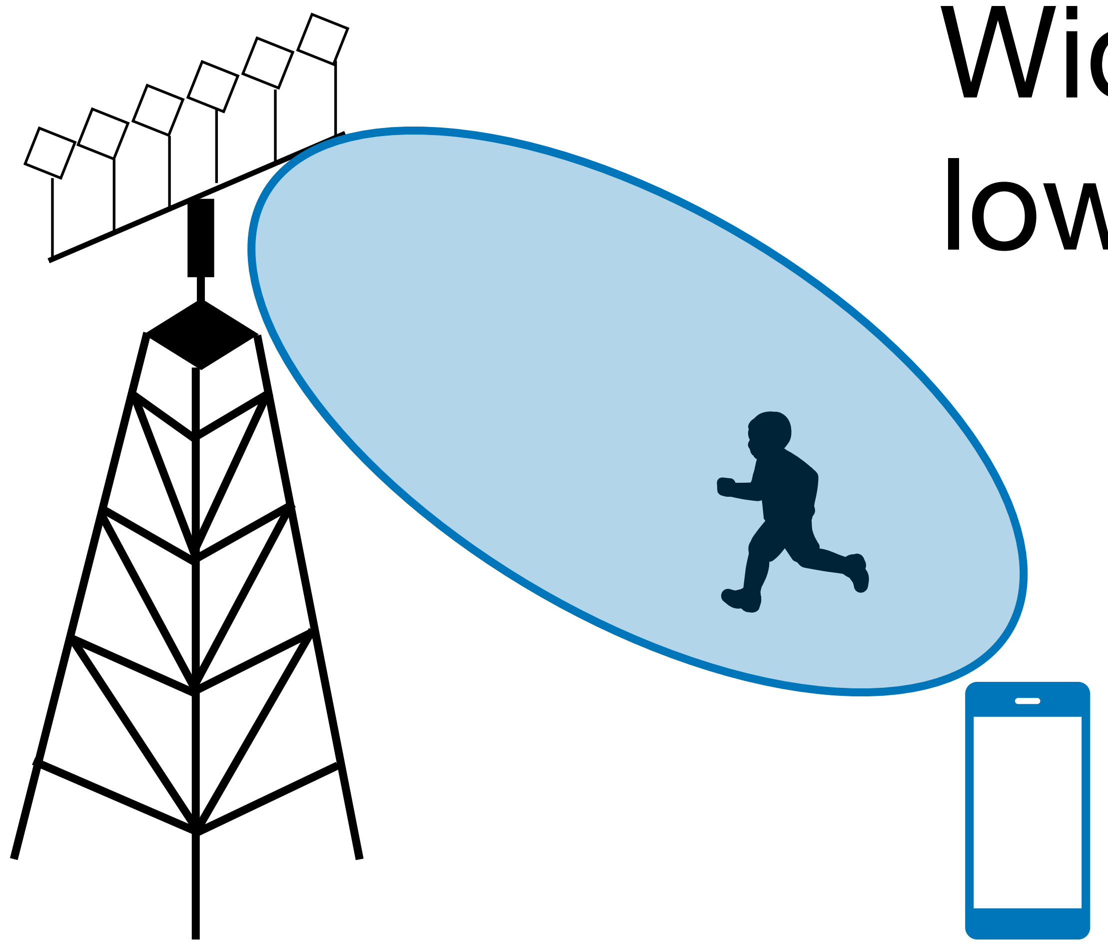

Wide beams in low-frequency

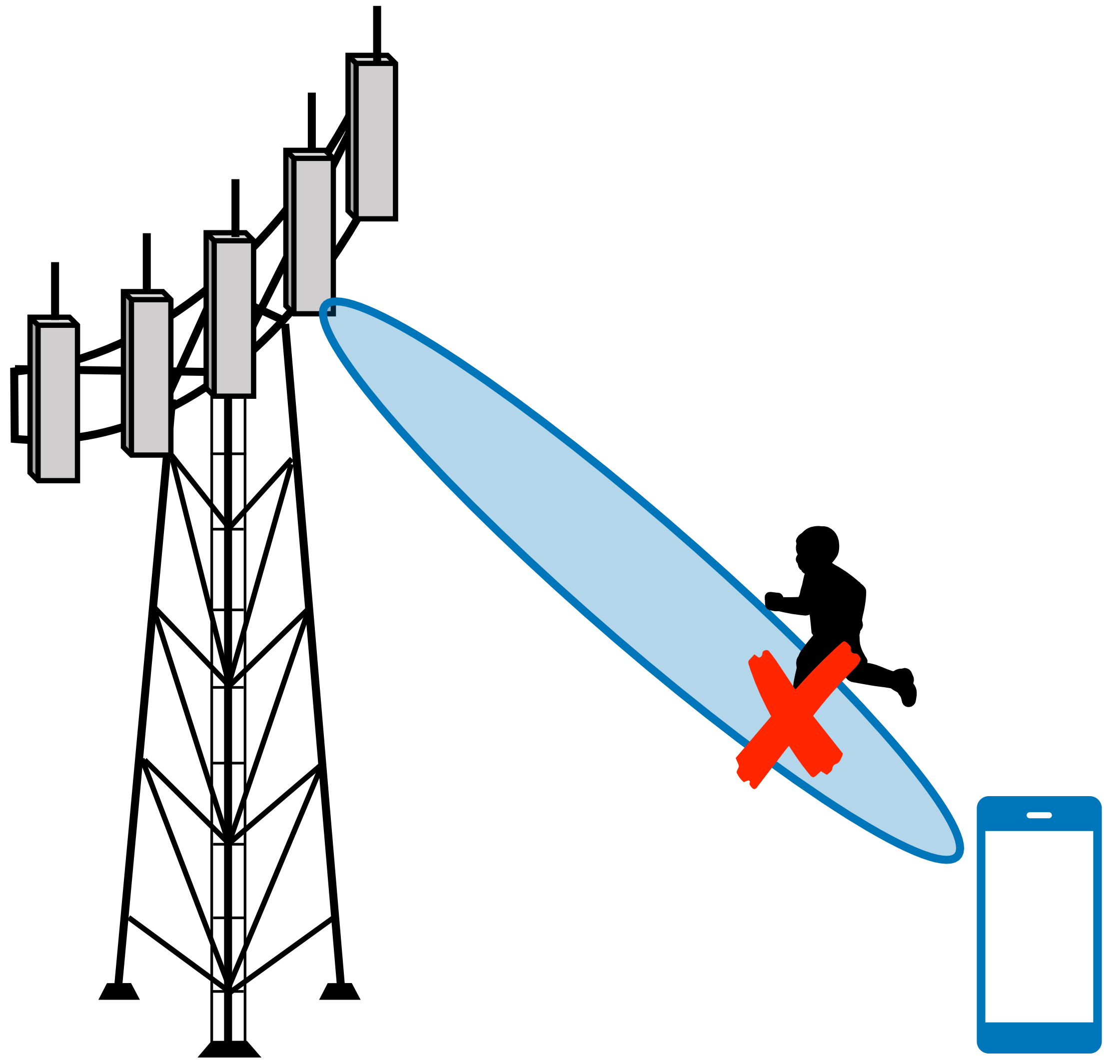

Narrow beams in high-frequency

Near-Field Communications

- **A large antenna aperture** for high directivity makes the signal's spherical wavefront non-negligible.
  - This near-field effect must be considered in beam design.

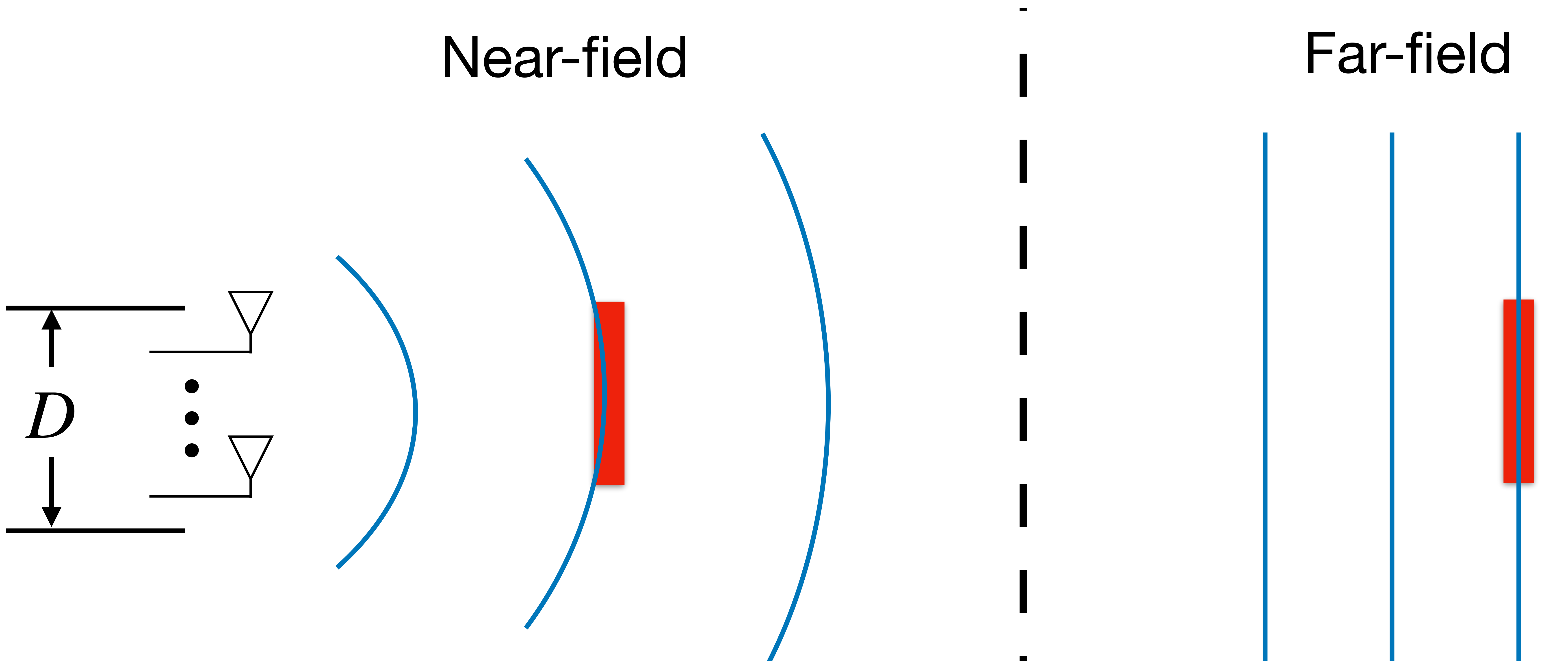

A reference point, which is proportional to D

Near-Field Beams

- Beam optimizations for the environment requires full CSI
  - Challenge: high-dimensional, near-field channels make CSI estimation hard
  - Any nice beam solely using *partial side information*?

Near-Field Beams

- Beam optimizations for the environment requires full CSI
  - Challenge: high-dimensional, near-field channels make CSI estimation hard
  - Any nice beam solely using *partial side information*?

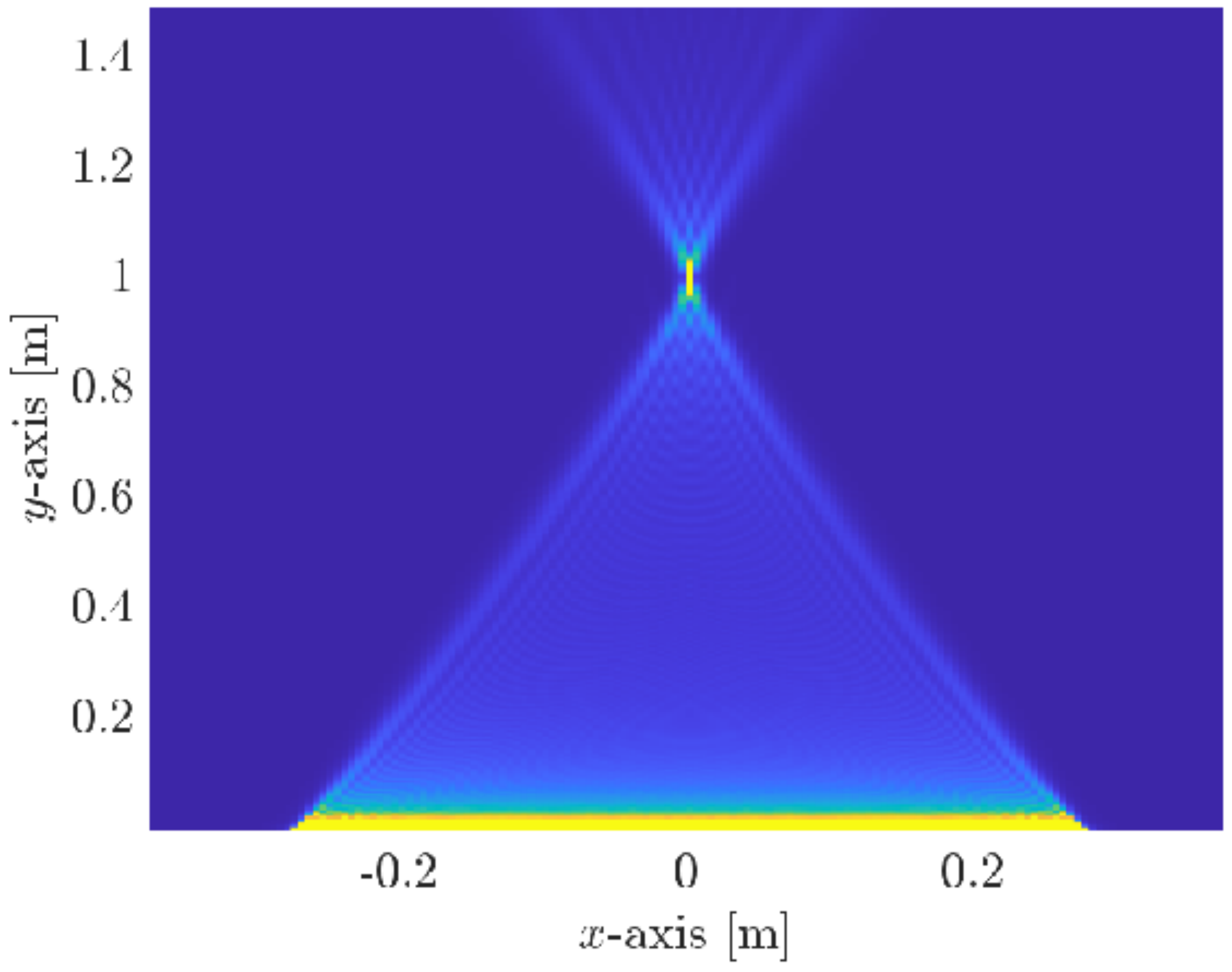

Beam focusing with UE's position

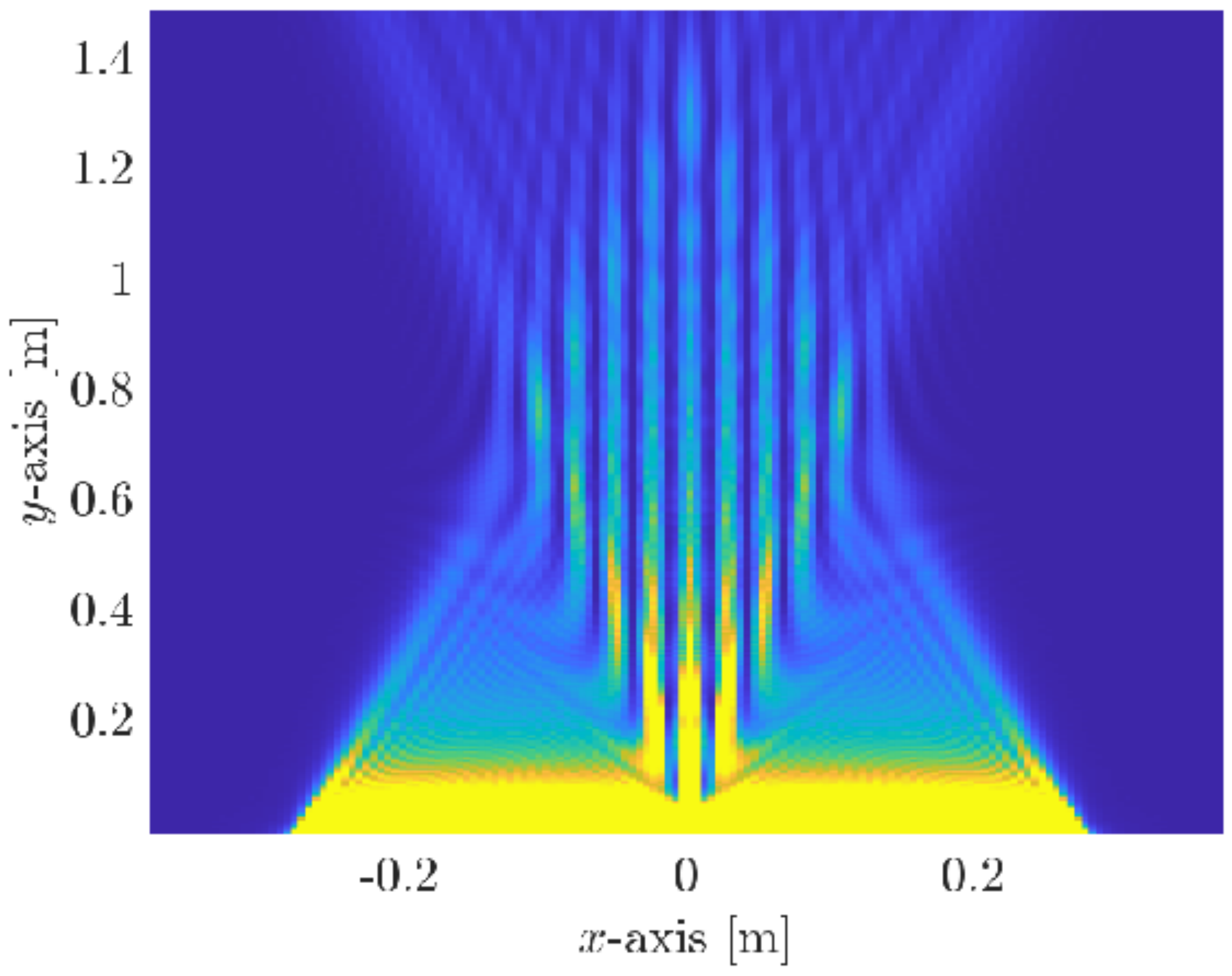

Bessel beam with UE's angle

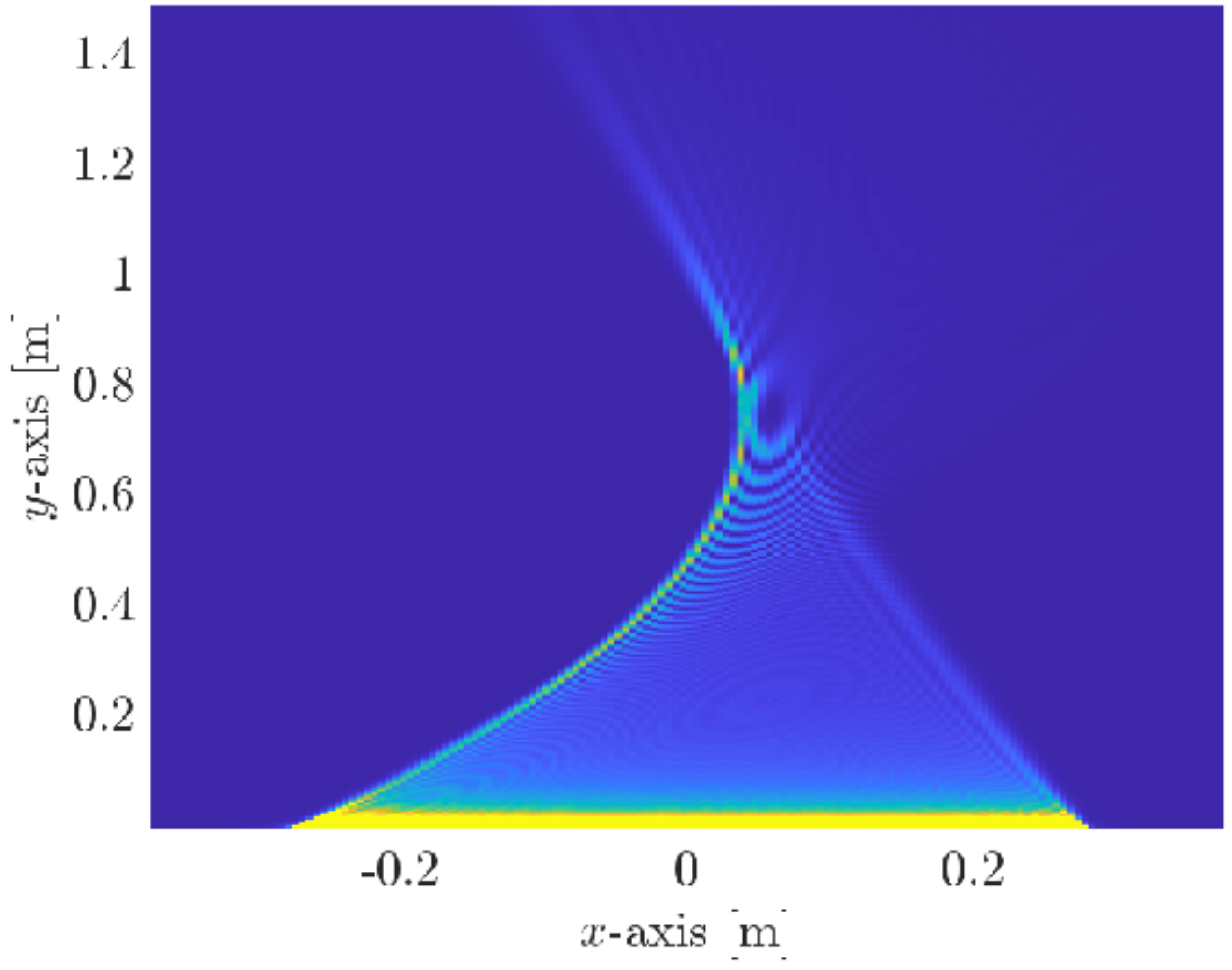

Curving beam with UE's and blocker's positions

Necessity of Wavefront Engineering

AWCC Advanced Wireless and Communication Research Center

- No beam is universally optimal [TWC'24]
  - Necessity of wavefront hopping via phased array
- Bessel beam steering [Bal'24]
  - Toward the desired azimuth and elevation
  - lacks a closed-form expression of phase distribution
- Curving beam steering [TWC'25]
  - Analyses on propagation and beam design for a known user position
  - No trajectory optimization to avoid obstacles

[TWC'24] V. Petrov et al., "Wavefront hopping: An enabler for reliable and secure near field terahertz communications in 6G and beyond," IEEE Wireless Commun., vol. 31, no. 1, pp. 48–55, Feb. 2024.
[Bal'24] A. Simoncic, and et al.,"Near-field beam steering with planar antenna array," in Proc. 7th Int. BalkanCom, Jun. 2024, pp. 31–36
[TWC'25] S. Droulias, and et al., "Bending beams for 6G near-field communications," IEEE TWC., vol.24, no.2, pp. 1467--1480, Feb. 2025.

Today's Talk

- First part:
  - Near-field beam generation using uniform linear array (ULA)
  - Closed-form phase distributions of near-field beams
  - Properties and conditions of Bessel beam generation

arXiv Paper

- Second part:
  - Full-digital extremely-large (XL-) MIMO systems
  - Joint channel and data estimation for multiuser XL-MIMO

arXiv Paper

Today's Talk

- **First part:**
  - **Near-field beam generation using uniform linear array (ULA)**
  - **Closed-form phase distributions of near-field beams**
  - **Properties and conditions of Bessel beam generation**

arXiv Paper

- Second part:
  - Full-digital extremely-large (XL-) MIMO systems
  - Joint channel and data estimation for multiuser XL-MIMO

arXiv Paper

System Model

- Single propagation with a uniform linear array with N antenna elements
  - Manipulate the phases of phase-shifters ϕ_n
  - The phase can be decomposed into $\phi_n = kd_n$ where k is the wavenumber and d_n is the minimum distance between the n-th antenna element and the wavefront function.

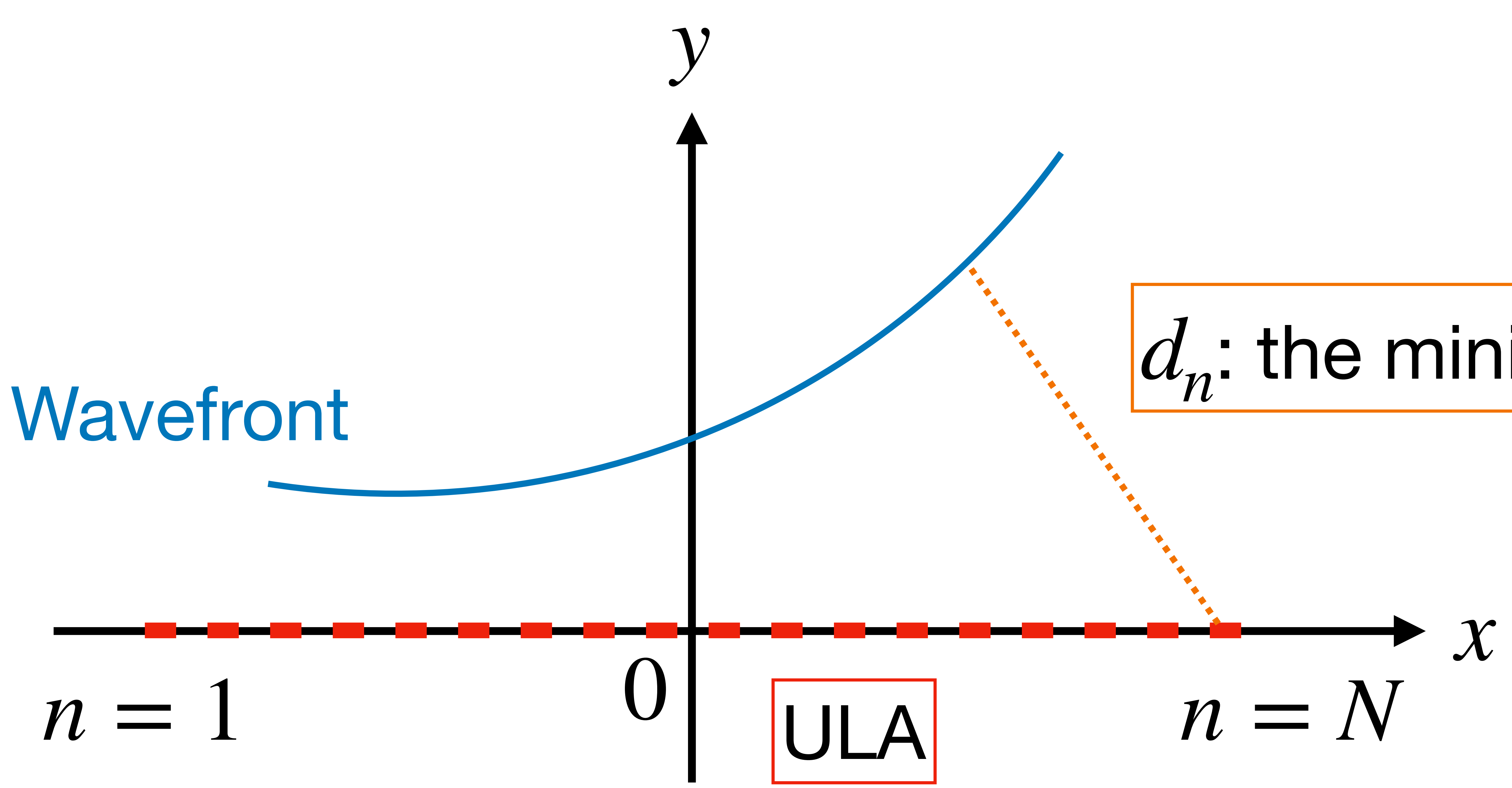

Wavefront Function of Bessel Beam

- A conical wavefront of an antenna array generates a Bessel beam [Phys'87]
  - A conical wavefront is described by an absolute function

$$f_{\mathrm{w}}(x) = \tan \alpha \,|\, x \,|$$

Hyper-parameter (c.t. beam-width)

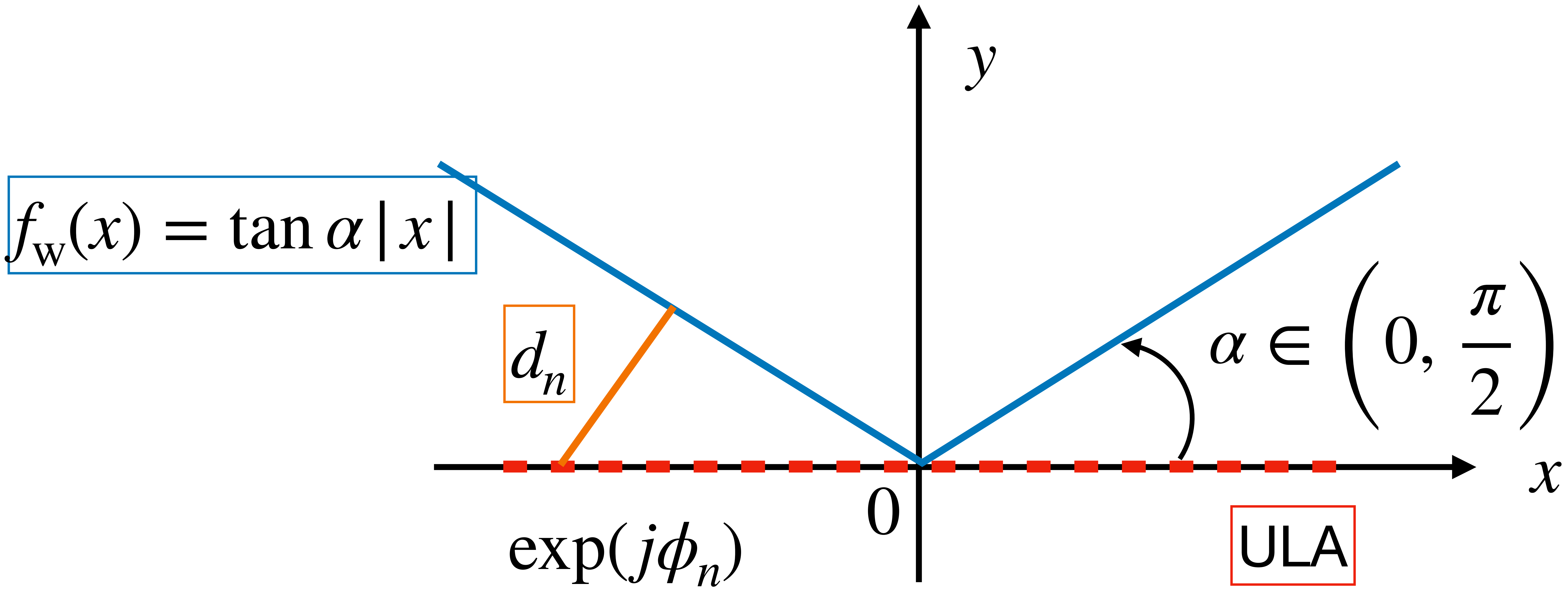

[Phys'87] J. Durnin et al.,"Diffraction-free beams," Phys. Rev. Lett., vol.58, pp.1499-1501, Apr. 1987.

Closed Form Bessel Beam Steering

- Consider a rotated coordinate system (x', y') based on the desired angle θ_A
  - Define an absolute function based on the rotated coordinate system.

$$f_\mathrm{w}(x) = \begin{cases} \tan(\alpha - \theta_\mathrm{A})x, & \text{if } x \geq 0 \\ -\tan(\alpha + \theta_\mathrm{A})x, & \text{otherwise} \end{cases}$$

$$\phi_n = \begin{cases} k\,|\sin(\alpha - \theta_\mathrm{A})|\,x_{\mathrm{t},n}, & \text{if } x_{t,n} \geq 0 \\ -k\,|\sin(\alpha + \theta_\mathrm{A})|\,x_{\mathrm{t},n}, & \text{otherwise} \end{cases}$$

$x_{\mathrm{t},n}$: the position of the n-th element

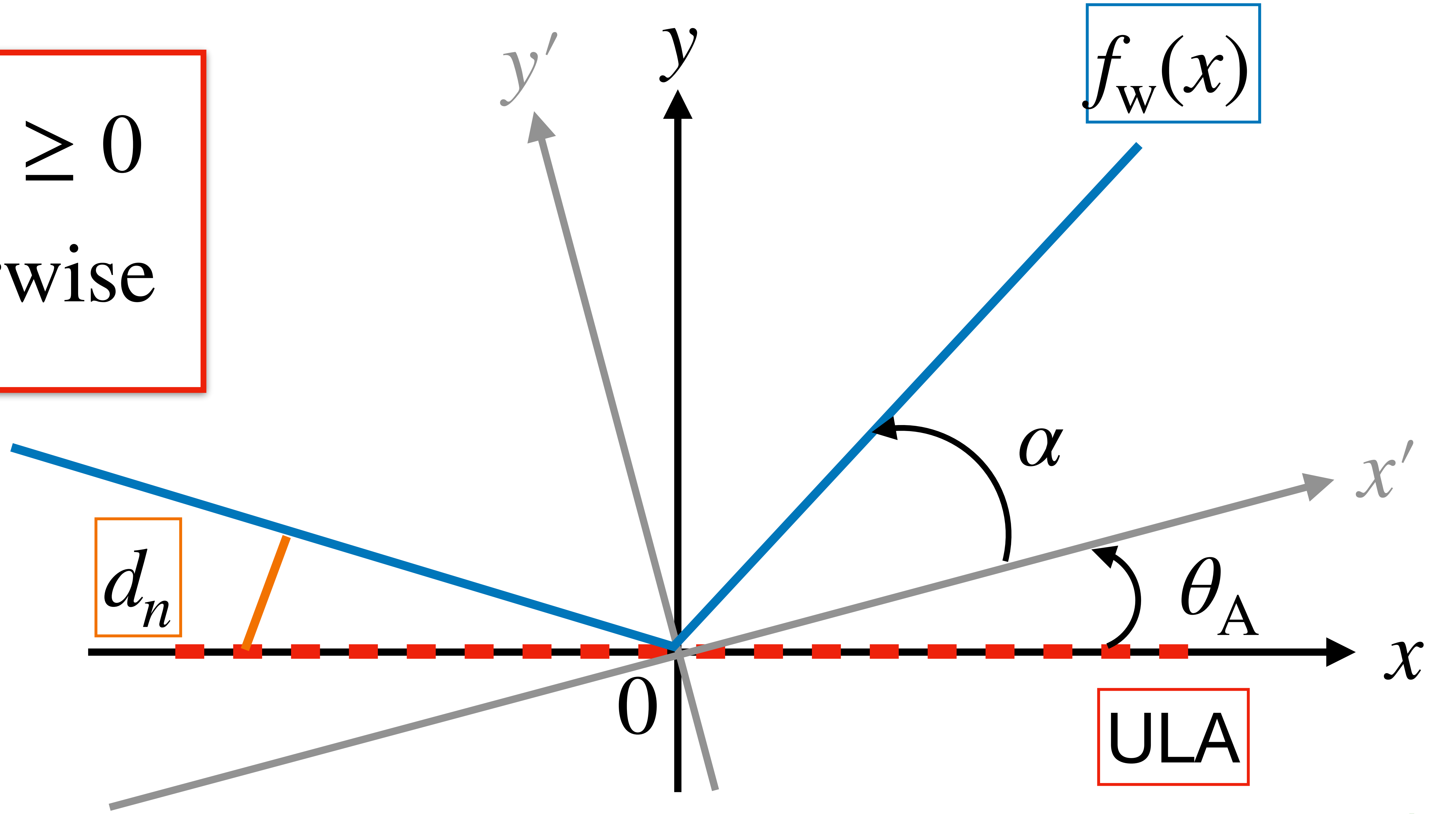

Necessary and Sufficient Condition for Steering

- The parameter α must satisfy $|\theta_\mathrm{A}| \le \alpha < \frac{\pi}{2} - |\theta_\mathrm{A}|$
  - Only the desired directions given by $\theta_\mathrm{A} \in (-\frac{\pi}{4}, \frac{\pi}{4})$ can be achieved.

$|\theta_\mathrm{A}| > \alpha$: reverse propagation

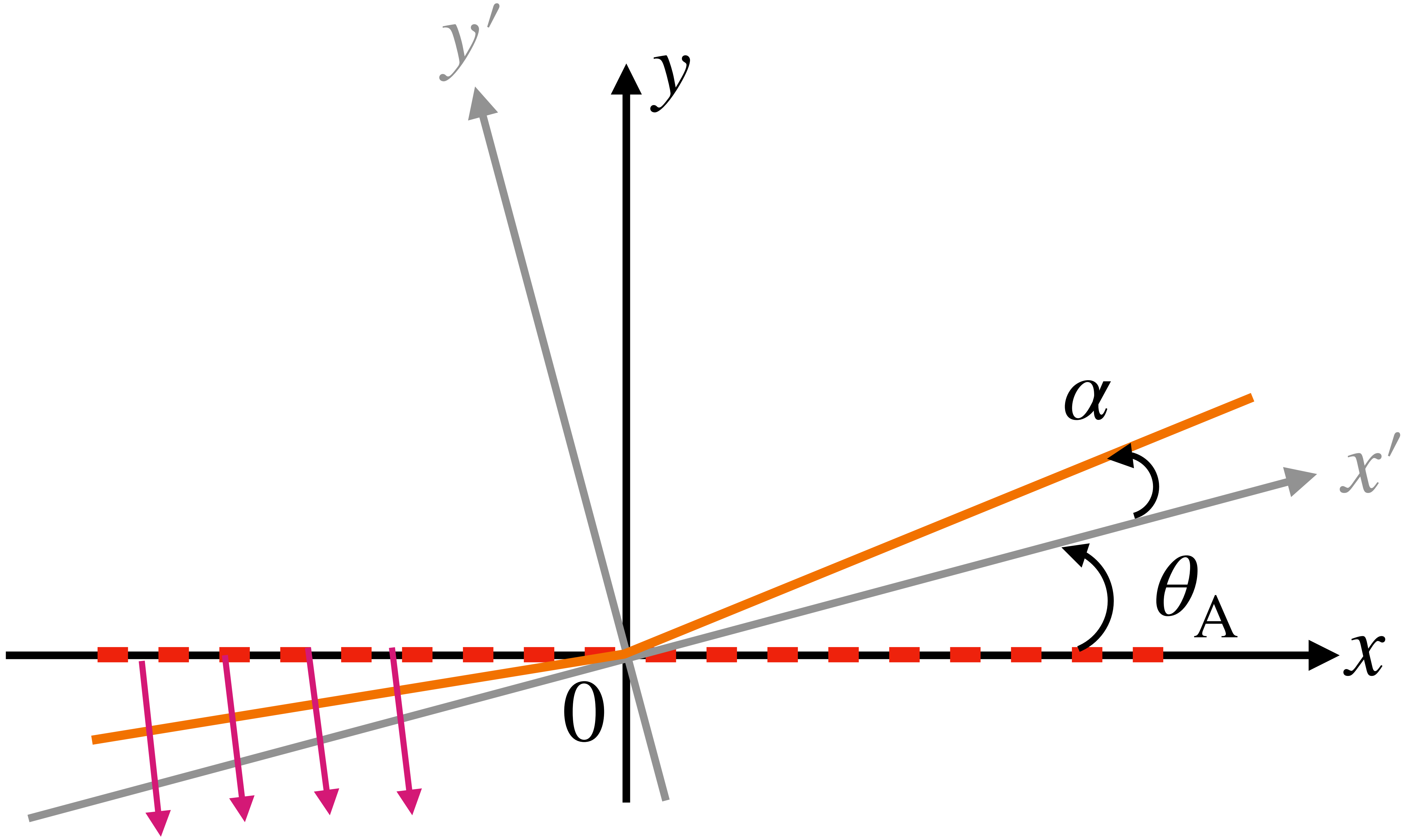

$\alpha \ge \frac{\pi}{2} - |\theta_\mathrm{A}|$: impossible wavefront

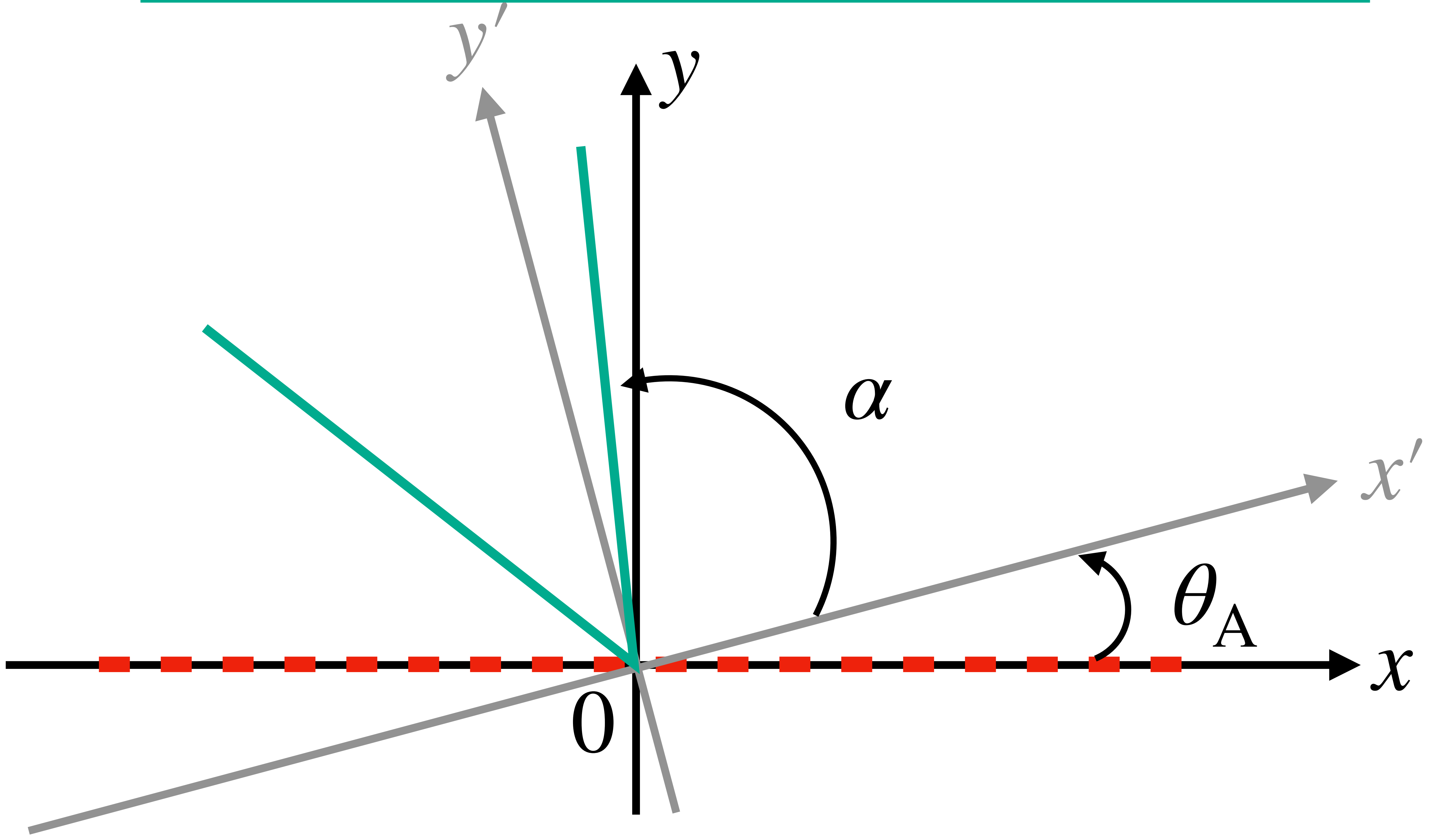

Maximum Propagation Distance

- Based on geometric optics [SIAM'66],
  - the maximum distance of the non-steering Bessel beam is given by $\frac{R}{\tan\alpha}$ [Phys'87].
  - In the steering case, the distances are given by

$$d_{\max} = \frac{R}{\tan\alpha}\frac{\cos(\alpha + |\theta_A|)}{\cos\alpha} < \frac{R}{\tan\alpha}$$

$$d_{\lim} = \frac{R}{\tan\alpha}\frac{\cos(\alpha - |\theta_A|)}{\cos\alpha} > \frac{R}{\tan\alpha}$$

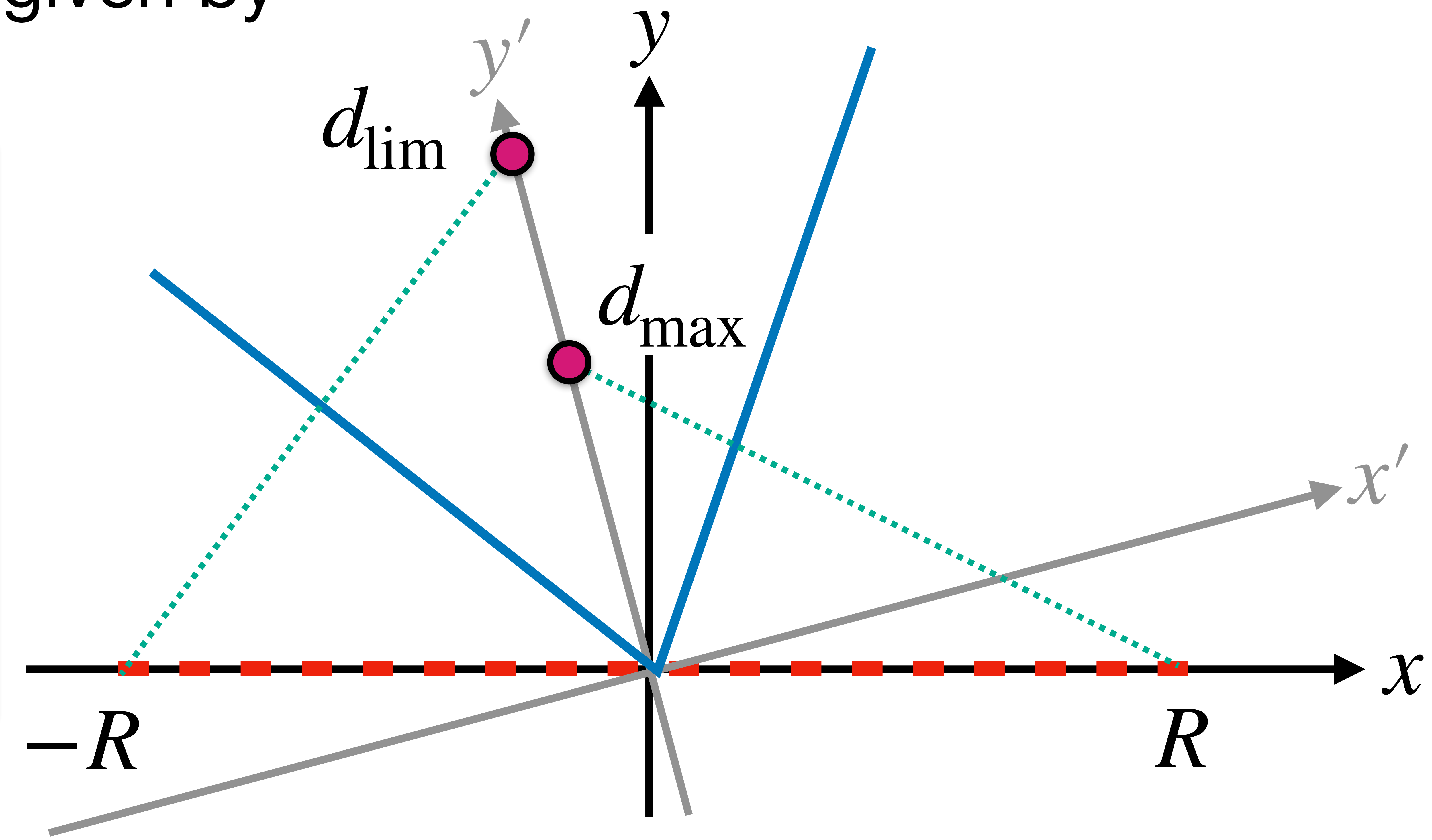

[SIAM'66] E. W. Marchand, "Electromagnetic theory and geometrical optics," SIAM Rev., vol.8, no.1, Jan. 1966.
[Phys'87] J. Durnin et al.,"Diffraction-free beams," Phys. Rev. Lett., vol.58, pp.1499-1501, Apr. 1987.

Self-Healing Capability

- Consider a rectangular obstacle in the 2D-plane
  - The rays from $x_{\mathrm{t},n} < x_{\mathrm{p}}^{\star}$ are blocked $(x_{\mathrm{t},n} > 0)$ / $x_{\mathrm{t},n} > x_{\mathrm{m}}^{\star}$ are blocked $(x_{\mathrm{t},n} < 0)$.
  - $x_{\mathrm{p}}^{\star} = \min_{x \in \mathscr{X}_{\mathrm{p}}} x, \ \mathscr{X}_{\mathrm{p}} \triangleq \{x \in \mathscr{X}_{\mathrm{arr}} \mid x > x_{\mathrm{r},1} + \tan(\alpha - \theta_{\mathrm{A}}) y_{\mathrm{f}}\}$
  - $x_{\mathrm{m}}^{\star} = \min_{x \in \mathscr{X}_{\mathrm{m}}} x, \ \mathscr{X}_{\mathrm{m}} \triangleq \{x \in \mathscr{X}_{\mathrm{arr}} \mid x < x_{\mathrm{r},2} - \tan(\alpha + \theta_{\mathrm{A}}) y_{\mathrm{f}}\}$

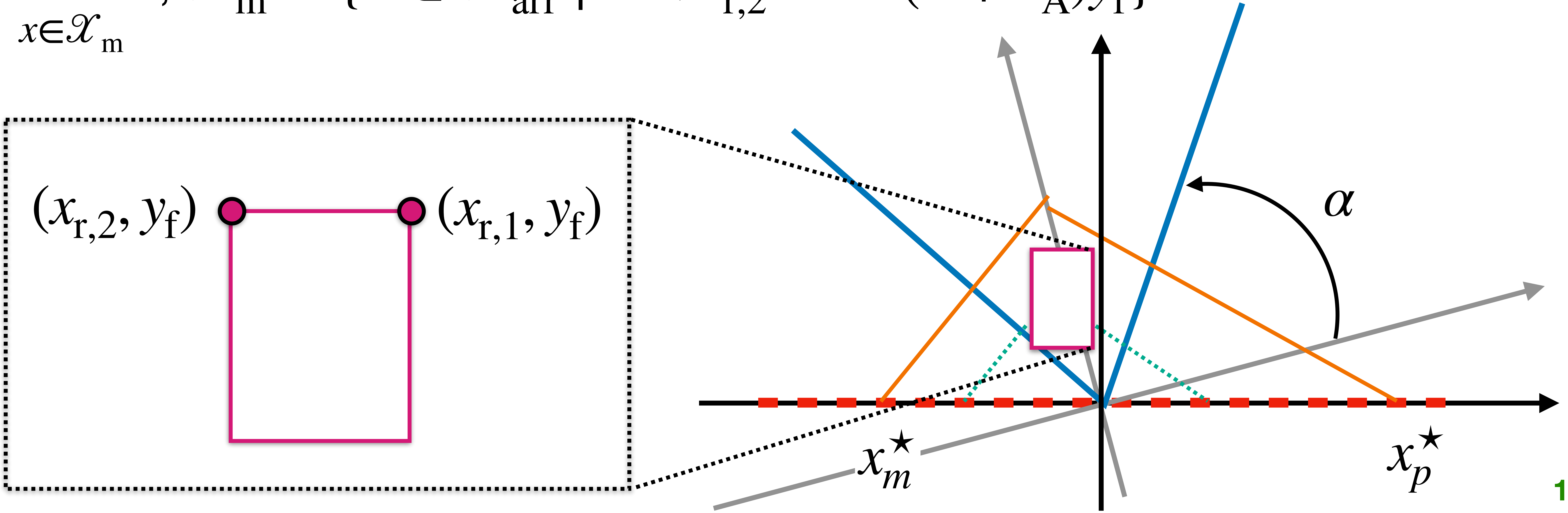

Maximum Distance vs Self-Healing Capability

- The smaller α leads to the longer maximum distance.
- The larger α leads to the higher self-healing capability.

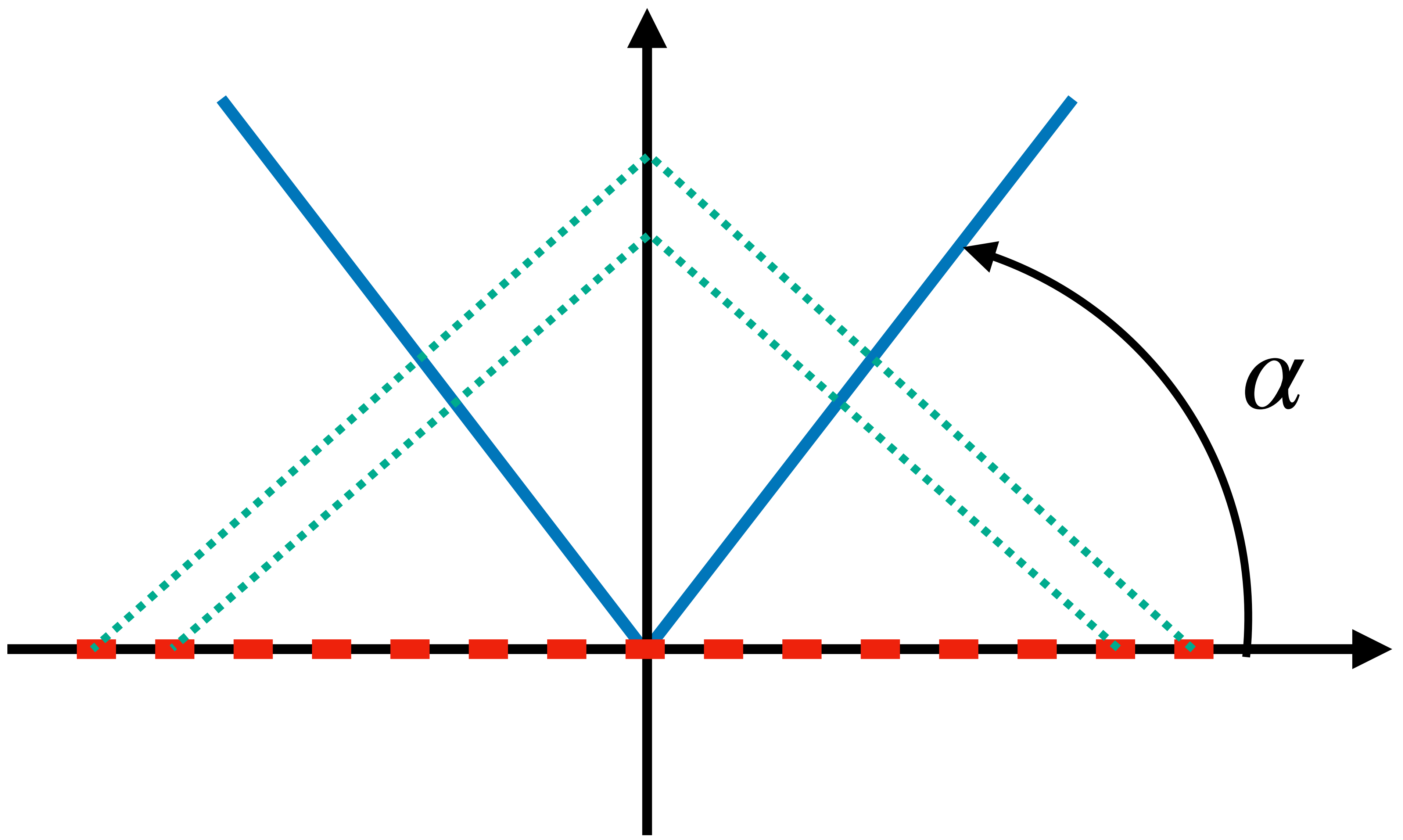

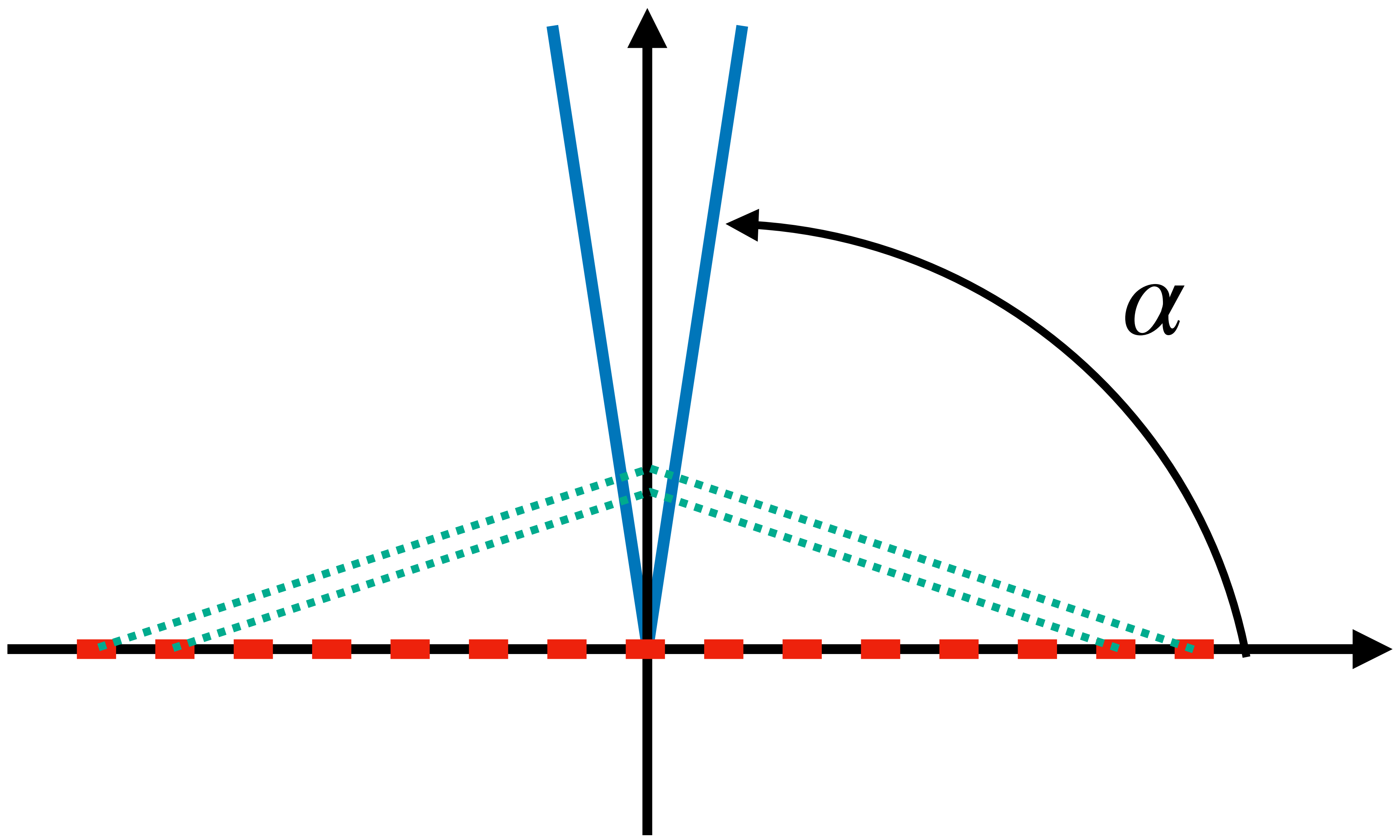

- Any way to improve both the propagation and self-healing capabilities?
  - **The possible approach is the adjustment of the antenna array.**

Adjustment of Antenna Array for Bessel Beams

AWCC Advanced Wireless and Communication Research Center

□ Increasing the number of antennas to achieve the distance $d_{\max,d}$ with the fixed α

- From $\frac{R}{\tan\alpha}\frac{\cos(\alpha+|\theta_\mathrm{A}|)}{\cos\alpha} \geq d_{\mathrm{max,d}}$, where $R = (N-1)\Delta/2$
- the minimum number of antenna elements is $N = \left\lceil 2d_{\mathrm{max,d}}\frac{\sin\alpha}{\Delta\cos(\alpha+|\theta_\mathrm{A}|)}+1\right\rceil$.

  $\lceil \cdot \rceil$: a ceiling function

□ Increasing the antenna spacing to achieve the distance $d_{\max,d}$ with the fixed α

- $\Delta = 2d_{\mathrm{max,d}}\frac{\sin\alpha}{(N-1)\cos(\alpha+|\theta_\mathrm{A}|)}$
- However, **the sampling theorem in the spatial domain** should be satisfied.

Antenna Spacing Condition from Sampling Theorem

- Since the ULA is located on the x-axis, the sampling theorem is $\Delta < \frac{\pi}{k_x}$ [TSP'22],
  - $\Delta < \frac{\lambda}{2}\frac{1}{\sin(\alpha + |\theta_A|)}$ should be satisfy to properly generate Bessel beams
  - Under the necessary and sufficient condition, $\frac{1}{\sin(\alpha + |\theta_A|)} > 1$, which means **the ULA with the half-wavelength spacing can generate any Bessel beam.**

$$\theta_A > 0, \sin(\alpha + \theta_A) > \sin(\alpha - \theta_A)$$
$$\theta_A < 0, \sin(\alpha + \theta_A) < \sin(\alpha - \theta_A)$$

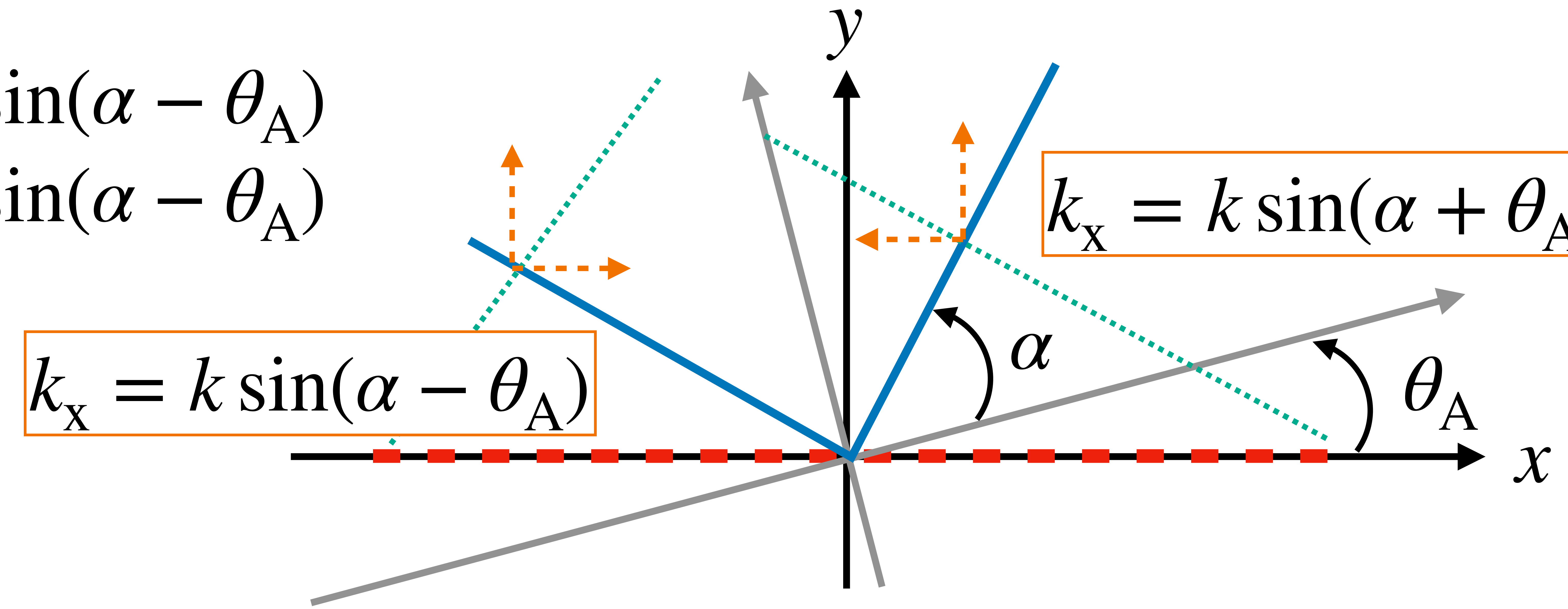

[TSP'22] A. Pizzo, and et al, "Nyquist sampling and degrees of freedom of electromagnetic fields," IEEE Trans. Sig. Process., 2022

Curving Beams

- Consider design of curving beams. In ULA systems,
  - any trajectory described by convex or concave functions can be achieved.
  - only the parabolic trajectory is considered to simply the discussion, where the trajectory function is given by $f_{\mathrm{t}}(y) = \beta(y-p)^2 + q$.
  - the envelope forms a curving beam.

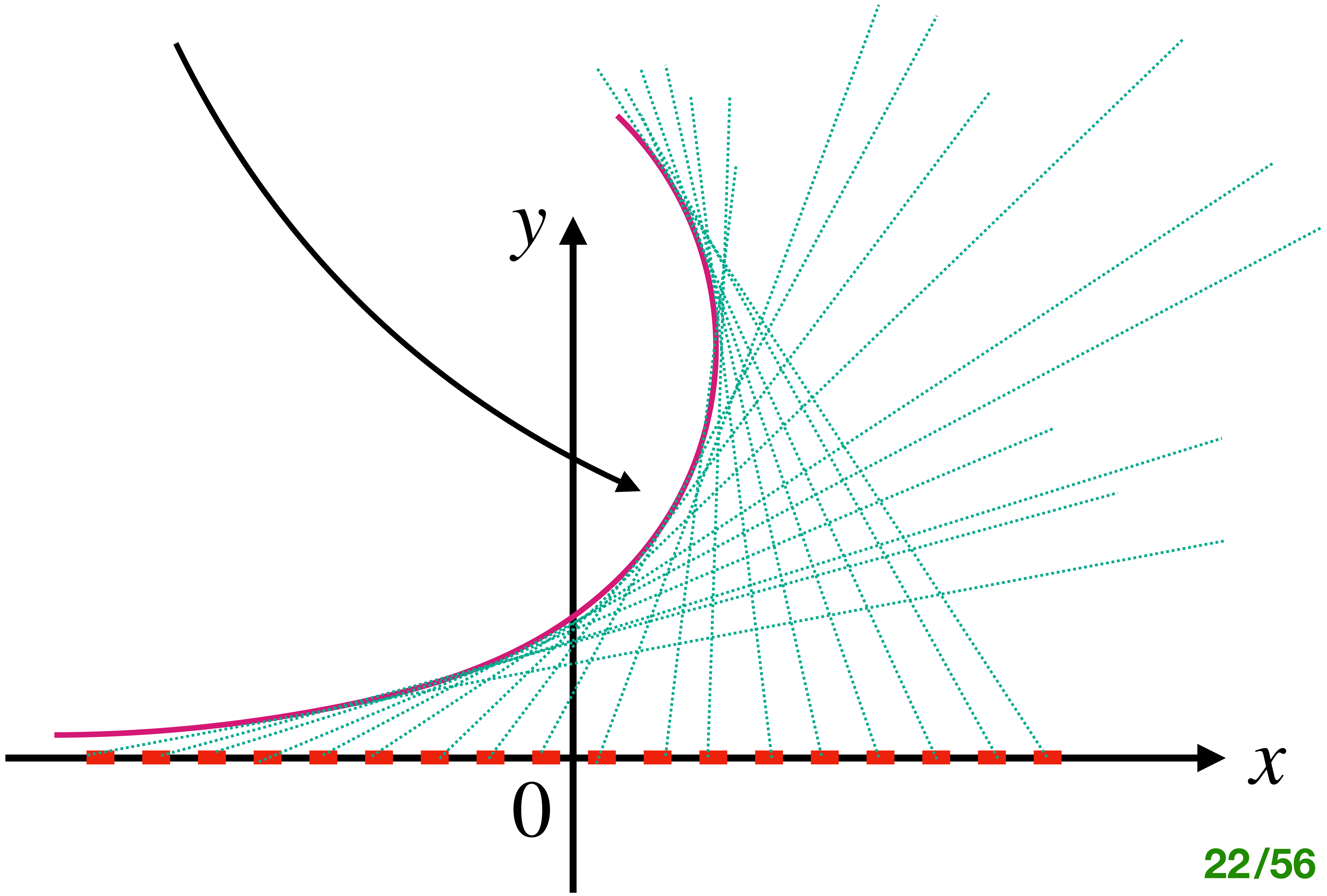

Parabolic Trajectory to a User

- Consider a user, whose position is $(x_{\mathrm{u}}, y_{\mathrm{u}})$.
  - The parameters β, p, q should satisfy $x_{\mathrm{u}} = \beta(y_{\mathrm{u}} - p)^2 + q$, which leads to

$q = x_{\mathrm{u}} - \beta(y_{\mathrm{u}} - p)^2$ and

$$f_{\mathrm{t}}(y) = \beta(y^2 - y_{\mathrm{u}}^2) - 2\beta p(y - y_{\mathrm{u}}) + x_{\mathrm{u}}$$

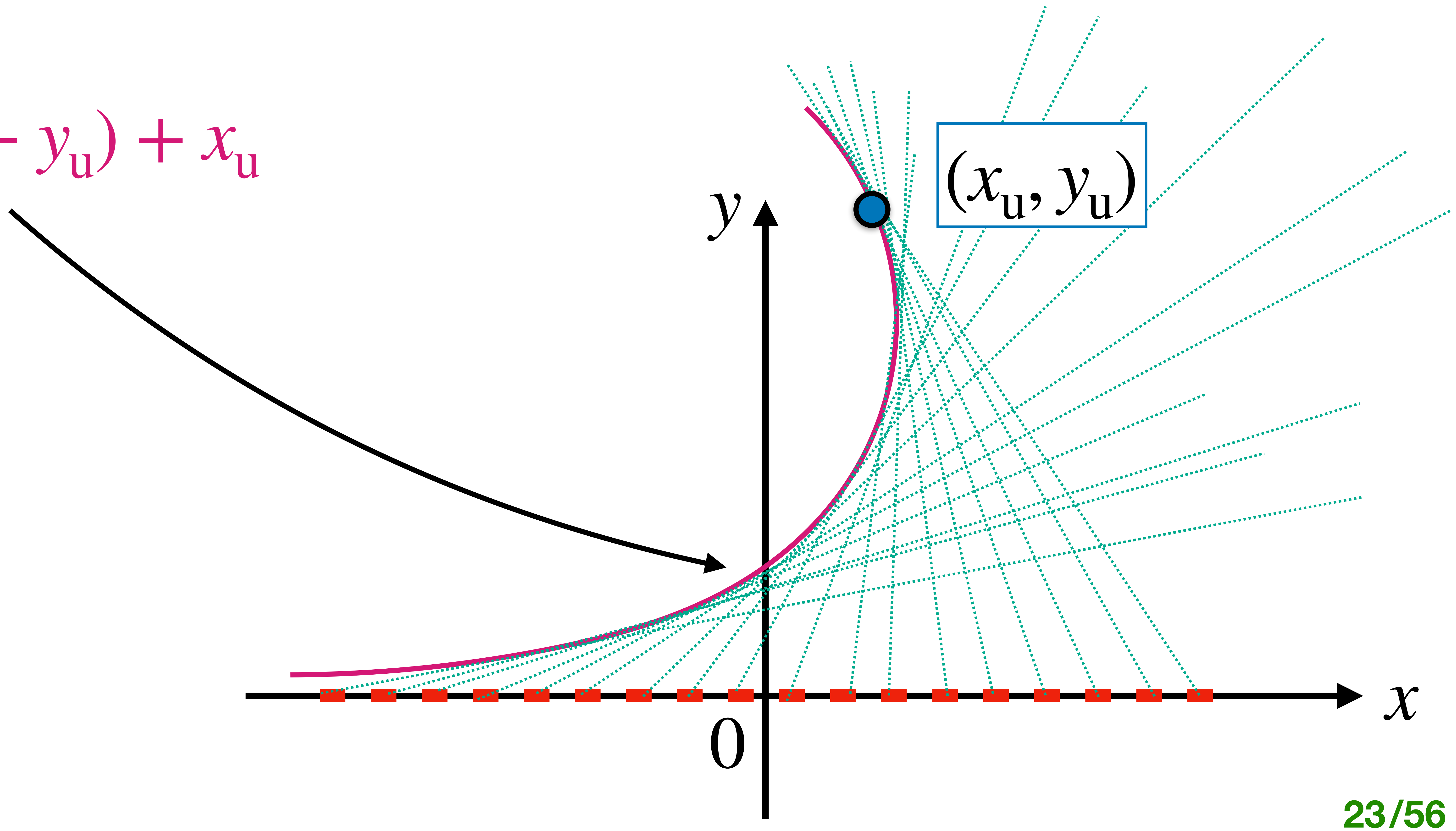

Phase Distribution of Parabolic Trajectory

- Based on the study of [TWC'25], the phase at the n-th element is given by

$$\phi_n = k\left\{\frac{\log(\sqrt{c_1} - c_2)}{4|\beta|} - \left(p + \sqrt{\frac{\beta p^2 + q - x_{\mathrm{t},n}}{\beta}}\right)\frac{\sqrt{c_1}}{2}\right\}$$

where

$$c_1 = 4\beta^2 p^2 + 4\beta(\beta p^2 + q - x_{\mathrm{t},n}) - 8\beta^2 p\sqrt{\frac{\beta p^2 + q - x_{\mathrm{t},n}}{\beta}} + 1$$

$$c_2 = \left(2\beta^2 p - 2\beta^2\sqrt{\frac{\beta p^2 + q - x_{\mathrm{t},n}}{\beta}}\right)\frac{1}{|\beta|}$$

- From $q = x_\mathrm{u} - \beta(y_\mathrm{u} - p)^2$, **the design of curving beams is equivalent to the design of the parameters β and p.**

[TWC'25] S. Droulias, and et al., "Bending beams for 6G near-field communications," IEEE TWC., vol.~24, no.2, pp. 1467-1480, Feb. 2025.

Problem Formulation

- Joint optimization of the parameters and the effective aperture of the ULA to avoid the known obstacle

$$\text{Find } \beta > 0,\ p,\ x_{\text{adj}}$$

$$\text{subject to } f_{\text{t}}(y_{\text{n}}) \le x_{\text{r},2}$$

$$f_{\text{t}}(y_{\text{f}}) \le x_{\text{r},2}$$

$$y_{\text{t, min}} \le y_{\text{u}}$$

$$y_{\text{u}} \le y_{\text{t, max}}$$

$$x_{\text{adj}} \in \mathcal{X}_{\text{arr}}$$

$\mathcal{X}_{\text{cal}}$: the set of antenna positions

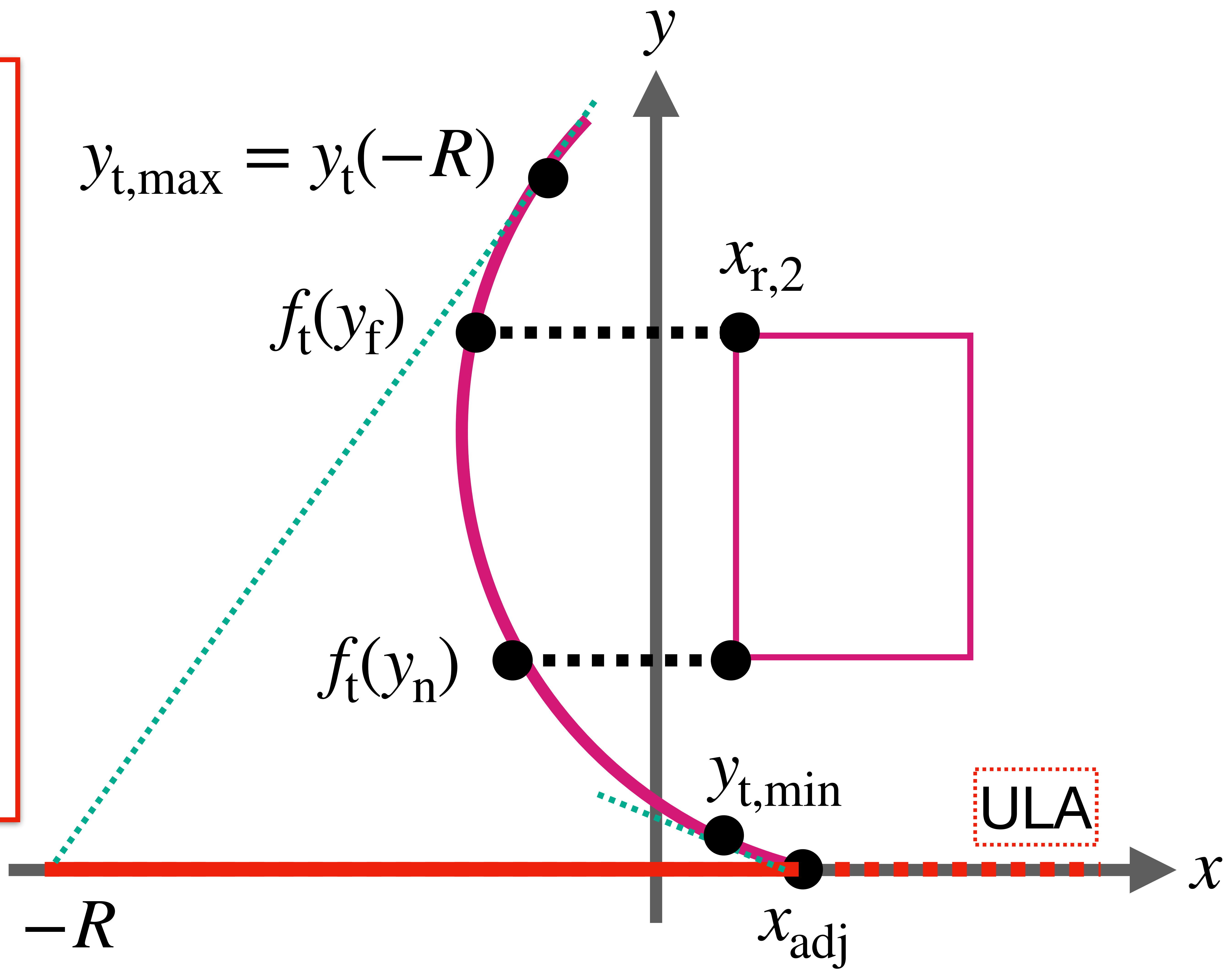

Closed-Form Solutions

- Based on the Lagrangian method,
  the possible candidates of the closed-form solutions are given by

$$
(\beta, \tilde{p}, x_{\mathrm{adj}}) = \begin{cases}
\left(\frac{-(x_{\mathrm{r},2}-x_{\mathrm{u}})}{(y_{\mathrm{f}}-y_{\mathrm{u}})(y_{\mathrm{n}}-y_{\mathrm{u}})}, \frac{-(x_{\mathrm{r},2}y_{\mathrm{f}}-x_{\mathrm{u}}y_{\mathrm{f}}+x_{\mathrm{r},2}y_{\mathrm{n}}-x_{\mathrm{u}}y_{\mathrm{n}})}{2(y_{\mathrm{f}}-y_{\mathrm{u}})(y_{\mathrm{n}}-y_{\mathrm{u}})}, \frac{x_{\mathrm{r},2}y_{\mathrm{u}}^2+x_{\mathrm{u}}y_{\mathrm{f}}y_{\mathrm{n}}-x_{\mathrm{r},2}y_{\mathrm{f}}y_{\mathrm{u}}-x_{\mathrm{r},2}y_{\mathrm{n}}y_{\mathrm{u}}}{(y_{\mathrm{f}}-y_{\mathrm{u}})(y_{\mathrm{n}}-y_{\mathrm{u}})} \right) \\
\left(\frac{-(Ry_{\mathrm{f}}-Ry_{\mathrm{u}}+x_{\mathrm{u}}y_{\mathrm{f}}-x_{\mathrm{r},2}y_{\mathrm{u}})}{y_{\mathrm{u}}(y_{\mathrm{f}}-y_{\mathrm{u}})^2}, \frac{-(Ry_{\mathrm{f}}^2-Ry_{\mathrm{u}}^2+x_{\mathrm{u}}y_{\mathrm{f}}^2-2x_{\mathrm{r},2}y_{\mathrm{u}}^2+x_{\mathrm{u}}y_{\mathrm{u}}^2)}{2y_{\mathrm{u}}(y_{\mathrm{f}}-y_{\mathrm{u}})^2}, \frac{-(Ry_{\mathrm{f}}^2-x_{\mathrm{r},2}y_{\mathrm{u}}^2-Ry_{\mathrm{f}}y_{\mathrm{u}}+x_{\mathrm{u}}y_{\mathrm{f}}y_{\mathrm{u}})}{(y_{\mathrm{f}}-y_{\mathrm{u}})^2} \right) \\
\left(\frac{-(Ry_{\mathrm{n}}-Ry_{\mathrm{u}}+x_{\mathrm{u}}y_{\mathrm{n}}-x_{\mathrm{r},2}y_{\mathrm{u}})}{y_{\mathrm{u}}(y_{\mathrm{n}}-y_{\mathrm{u}})^2}, \frac{-(Ry_{\mathrm{n}}^2-Ry_{\mathrm{u}}^2+x_{\mathrm{u}}y_{\mathrm{n}}^2-2x_{\mathrm{r},2}y_{\mathrm{u}}^2+x_{\mathrm{u}}y_{\mathrm{u}}^2)}{2y_{\mathrm{u}}(y_{\mathrm{n}}-y_{\mathrm{u}})^2}, \frac{-(Ry_{\mathrm{n}}^2-x_{\mathrm{r},2}y_{\mathrm{u}}^2-Ry_{\mathrm{n}}y_{\mathrm{u}}+x_{\mathrm{u}}y_{\mathrm{n}}y_{\mathrm{u}})}{(y_{\mathrm{n}}-y_{\mathrm{u}})^2} \right) \\
\left(\frac{Ry_{\mathrm{f}}-Ry_{\mathrm{u}}-x_{\mathrm{u}}y_{\mathrm{f}}+x_{\mathrm{r},2}y_{\mathrm{u}}}{y_{\mathrm{f}}y_{\mathrm{u}}(y_{\mathrm{f}}-y_{\mathrm{u}})}, \frac{Ry_{\mathrm{f}}^2-Ry_{\mathrm{u}}^2-x_{\mathrm{u}}y_{\mathrm{f}}^2+x_{\mathrm{r},2}y_{\mathrm{u}}^2}{2y_{\mathrm{f}}y_{\mathrm{u}}(y_{\mathrm{f}}-y_{\mathrm{u}})}, R \right) \\
\left(\frac{Ry_{\mathrm{n}}-Ry_{\mathrm{u}}-x_{\mathrm{u}}y_{\mathrm{n}}+x_{\mathrm{r},2}y_{\mathrm{u}}}{y_{\mathrm{n}}y_{\mathrm{u}}(y_{\mathrm{n}}-y_{\mathrm{u}})}, \frac{Ry_{\mathrm{n}}^2-Ry_{\mathrm{u}}^2-x_{\mathrm{u}}y_{\mathrm{n}}^2+x_{\mathrm{r},2}y_{\mathrm{u}}^2}{2y_{\mathrm{n}}y_{\mathrm{u}}(y_{\mathrm{n}}-y_{\mathrm{u}})}, R \right) \\
\left(\frac{-(Ry_{\mathrm{f}}-Ry_{\mathrm{u}}+x_{\mathrm{u}}y_{\mathrm{f}}-x_{\mathrm{r},2}y_{\mathrm{u}})}{y_{\mathrm{u}}(y_{\mathrm{f}}-y_{\mathrm{u}})^2}, \frac{-(Ry_{\mathrm{f}}^2-Ry_{\mathrm{u}}^2+x_{\mathrm{u}}y_{\mathrm{f}}^2-2x_{\mathrm{r},2}y_{\mathrm{u}}^2+x_{\mathrm{u}}y_{\mathrm{u}}^2)}{2y_{\mathrm{u}}(y_{\mathrm{f}}-y_{\mathrm{u}})^2}, R \right) \\
\left(\frac{-(Ry_{\mathrm{n}}-Ry_{\mathrm{u}}+x_{\mathrm{u}}y_{\mathrm{n}}-x_{\mathrm{r},2}y_{\mathrm{u}})}{y_{\mathrm{u}}(y_{\mathrm{n}}-y_{\mathrm{u}})^2}, \frac{-(Ry_{\mathrm{n}}^2-Ry_{\mathrm{u}}^2+x_{\mathrm{u}}y_{\mathrm{n}}^2-2x_{\mathrm{r},2}y_{\mathrm{u}}^2+x_{\mathrm{u}}y_{\mathrm{u}}^2)}{2y_{\mathrm{u}}(y_{\mathrm{n}}-y_{\mathrm{u}})^2}, R \right) \\
\left(\frac{Ry_{\mathrm{f}}-Ry_{\mathrm{u}}-x_{\mathrm{u}}y_{\mathrm{f}}+x_{\mathrm{r},2}y_{\mathrm{u}}}{y_{\mathrm{u}}(y_{\mathrm{f}}-y_{\mathrm{u}})^2}, \frac{-(Ry_{\mathrm{u}}^2-Ry_{\mathrm{f}}^2+x_{\mathrm{u}}y_{\mathrm{f}}^2-2x_{\mathrm{r},2}y_{\mathrm{u}}^2+x_{\mathrm{u}}y_{\mathrm{u}}^2)}{2y_{\mathrm{u}}(y_{\mathrm{f}}-y_{\mathrm{u}})^2}, R \right) \\
\left(\frac{Ry_{\mathrm{n}}-Ry_{\mathrm{u}}-x_{\mathrm{u}}y_{\mathrm{n}}+x_{\mathrm{r},2}y_{\mathrm{u}}}{y_{\mathrm{u}}(y_{\mathrm{n}}-y_{\mathrm{u}})^2}, \frac{-(Ry_{\mathrm{u}}^2-Ry_{\mathrm{n}}^2+x_{\mathrm{u}}y_{\mathrm{n}}^2-2x_{\mathrm{r},2}y_{\mathrm{u}}^2+x_{\mathrm{u}}y_{\mathrm{u}}^2)}{2y_{\mathrm{u}}(y_{\mathrm{n}}-y_{\mathrm{u}})^2}, R \right)
\end{cases}
$$

$$\tilde{p} = \beta p$$

↓ Full exploitation of a ULA

The trajectories with negative curvatures can be designed in the same manner.

General Setup For Numerical Results

- Consider the 3D coordinate system
  - The ULA is modeled as the set of ideal dipole sources.
  - The central frequency is set to 140 [GHz]
  - Electric fields in the xy-plane are calculated by EM simulations.

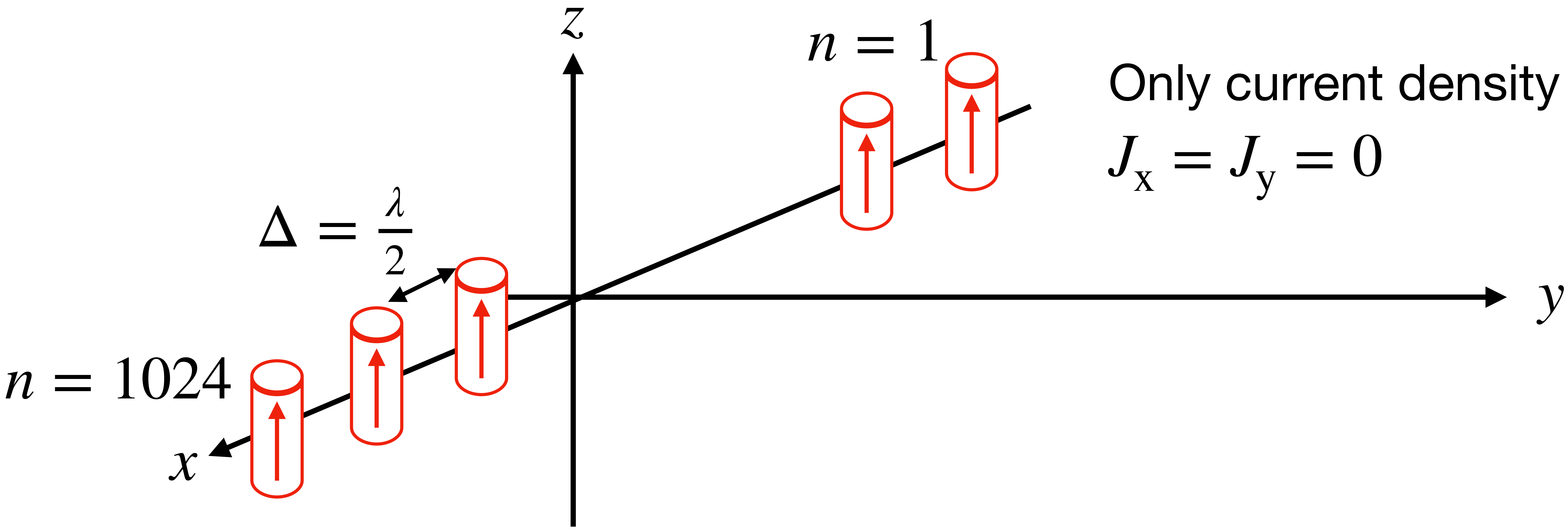

Only current density in the z-axis J_z

$J_x = J_y = 0$

Steering Bessel Beams

- The desired angle is set to $\theta_{\mathrm{A}} = 15$ [deg].
  - A smaller α achieves a longer propagation distance.

Magnitude of the electric field in the xy-plane [kV/m]

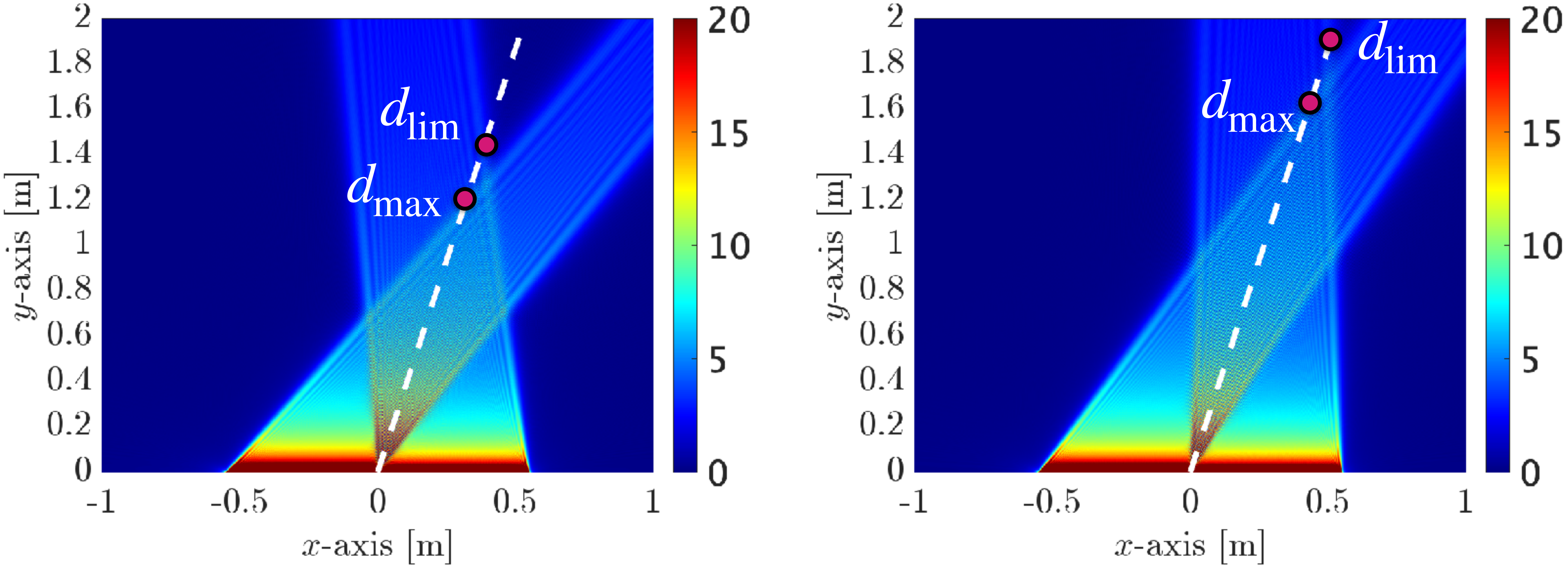

$\alpha = 20$ [deg] $\alpha = 15$ [deg]

Non-diffraction Propagation of Bessel Beams

- If $\alpha < |\theta_{\mathrm{A}}|$, *quasi-non-diffraction propagation cannot be achieved*.

$\alpha = 10$ [deg] ($< \theta_{\mathrm{A}} = 15$ [deg])

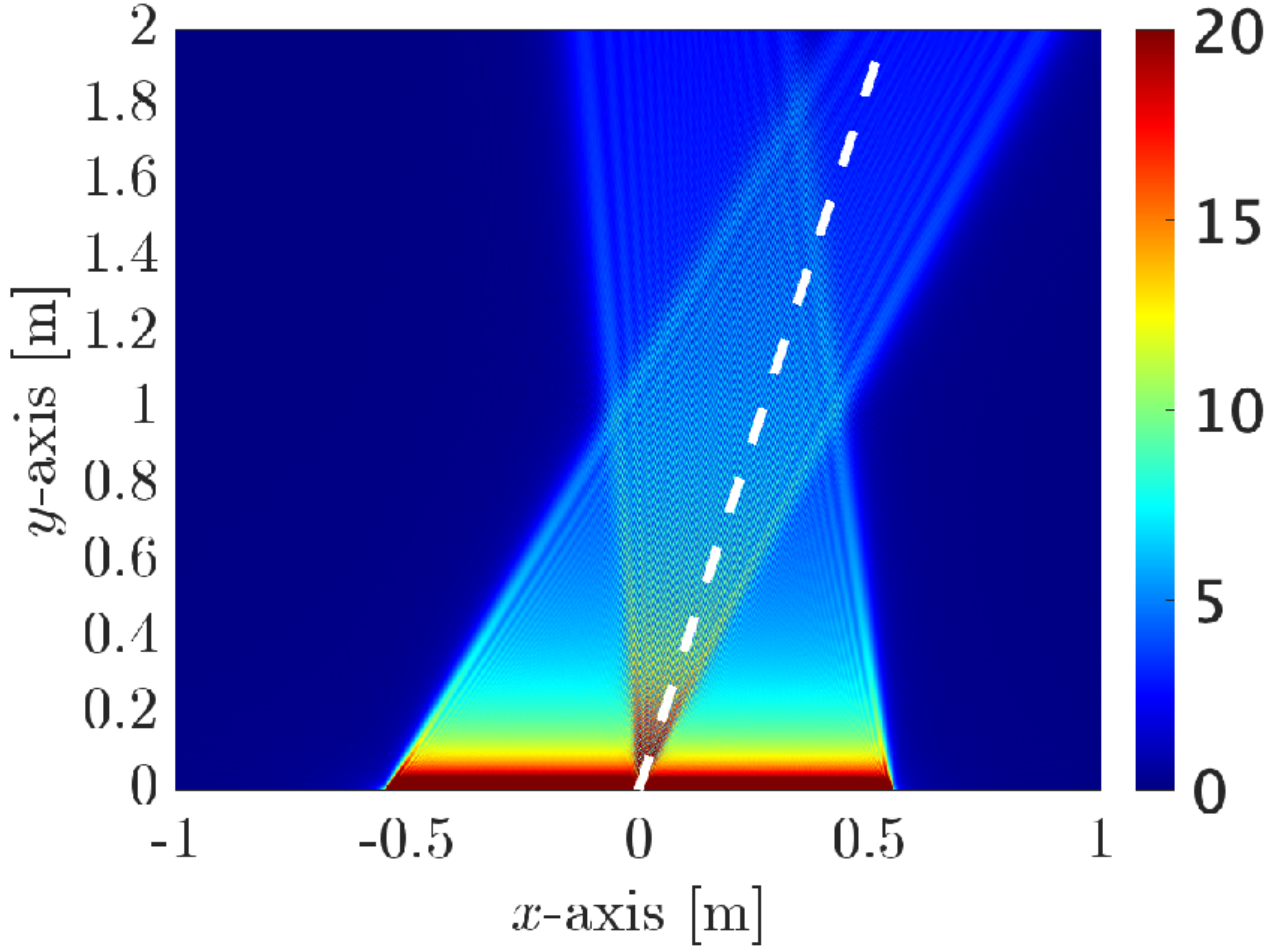

E-field along the desired direction

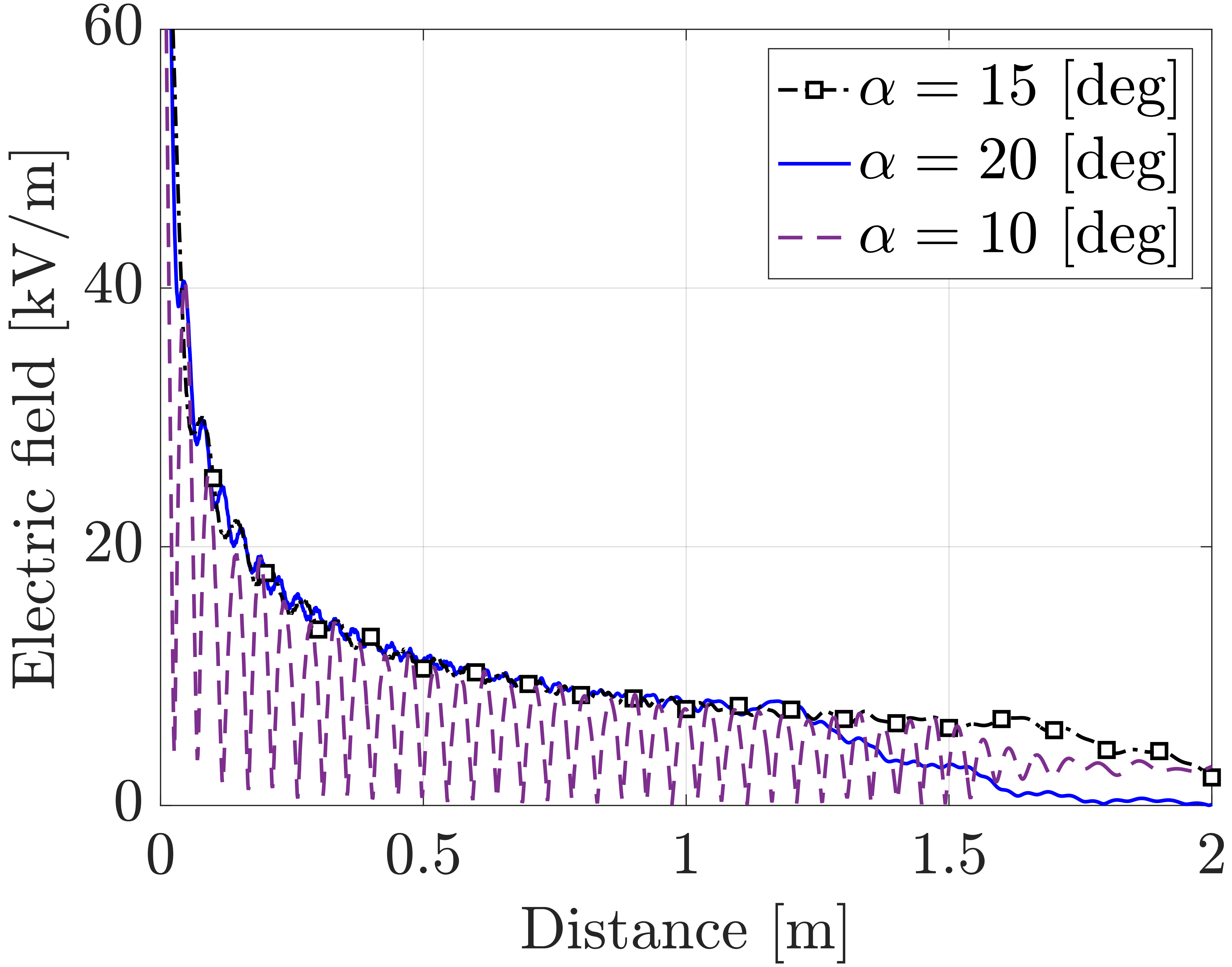

Sampling Theorem for Bessel Beams

- The desired distance is set to $d_{\max,d} = 4$ [m] with $\theta_\mathrm{A} = 15$ and $\alpha = 20$ [deg].
  - $\Delta < \frac{\lambda}{2}\frac{1}{\sin(\alpha + |\theta_\mathrm{A}|)} = 0.0018666\cdots$ should be satisfied.
- Grating lobes appear (right figure)
- Under the condition, the unintended beam does not interfere with the desired beam.

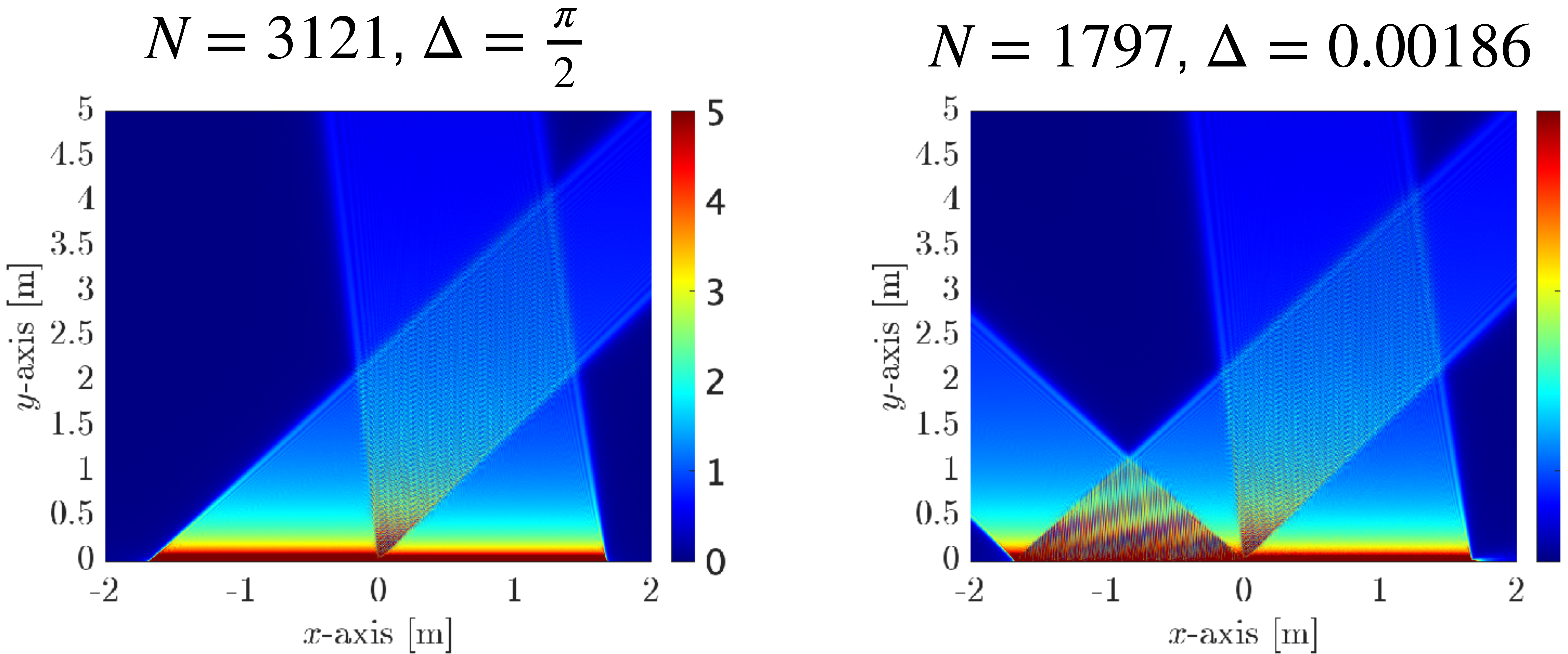

Wider Antenna Spacing

- The desired distance is set to $d_{\max,d} = 4$ [m] with $\theta_A = 15$ and $\alpha = 20$ [deg].
  - $\Delta < \frac{\lambda}{2}\frac{1}{\sin(\alpha + |\theta_A|)} = 0.0018666\cdots$ should be satisfied.
  - *Quasi-non-diffraction propagation cannot be achieved*.

$N = 899, \Delta = 0.00372$

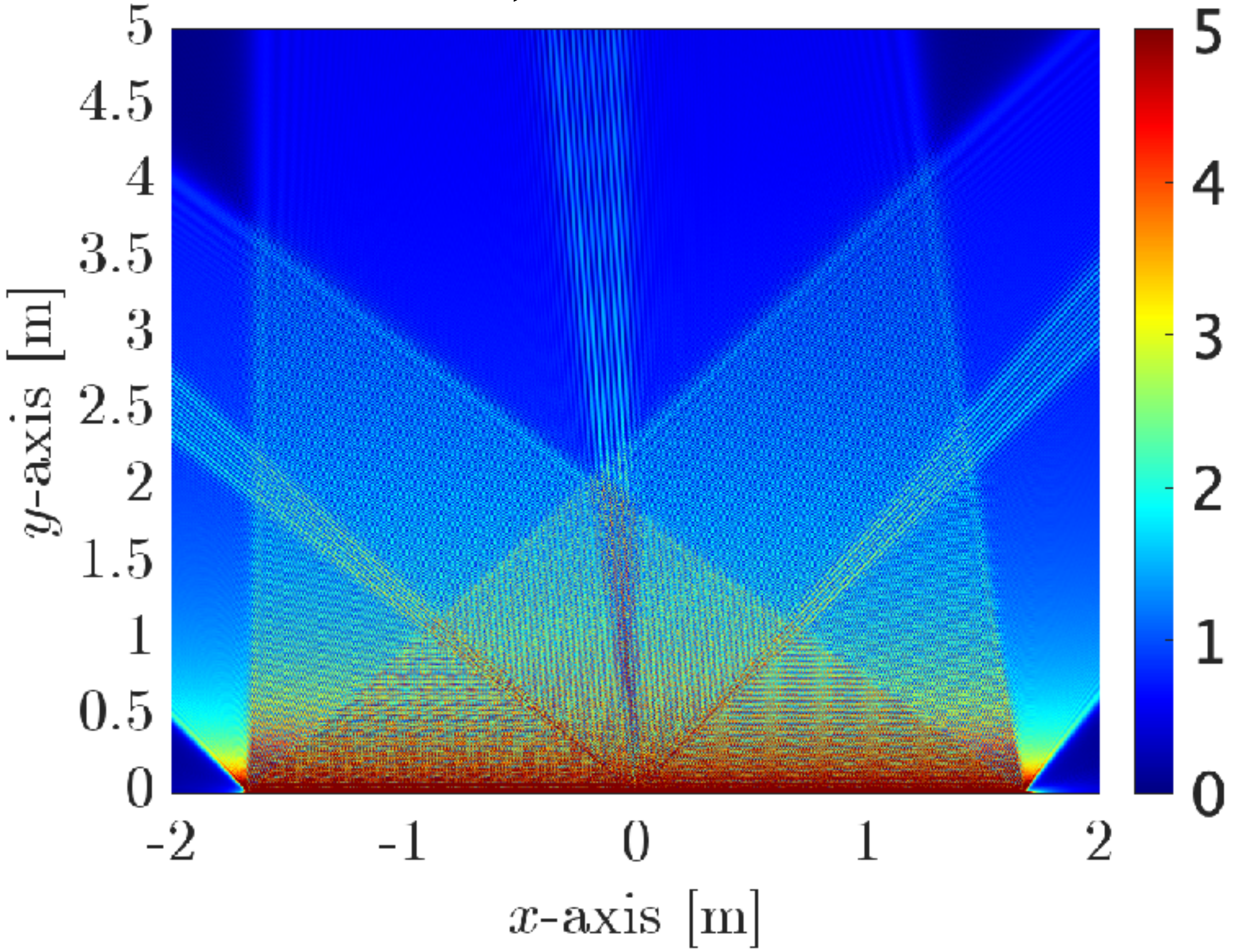

E-field along the desired direction

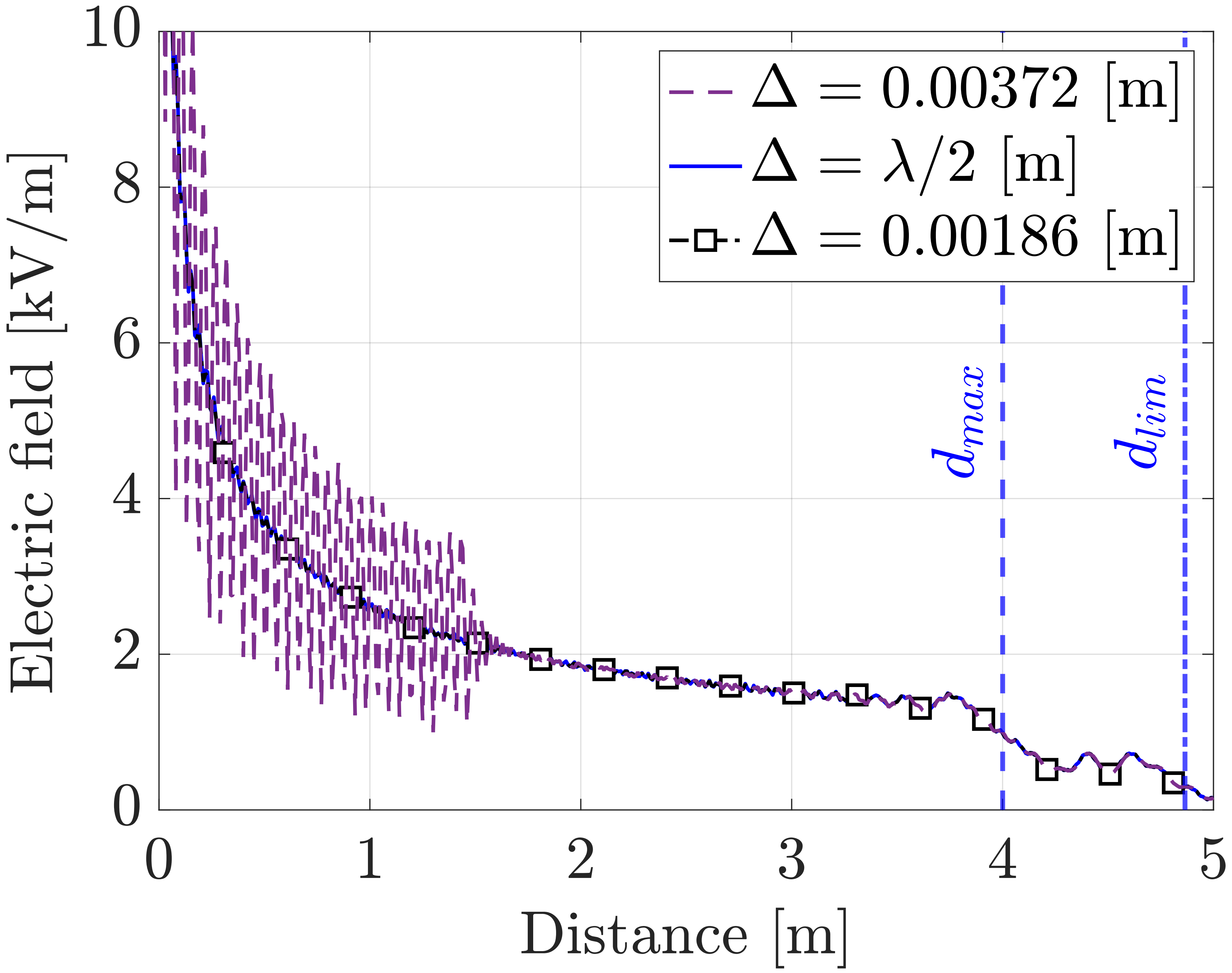

Numerical Results with Blockages

- The obstacle is modeled by a cuboid considering a human body.
  - Assume a perfect electric conductor.
  - The uniform theory of diffraction is used to evaluate the blockage effects.

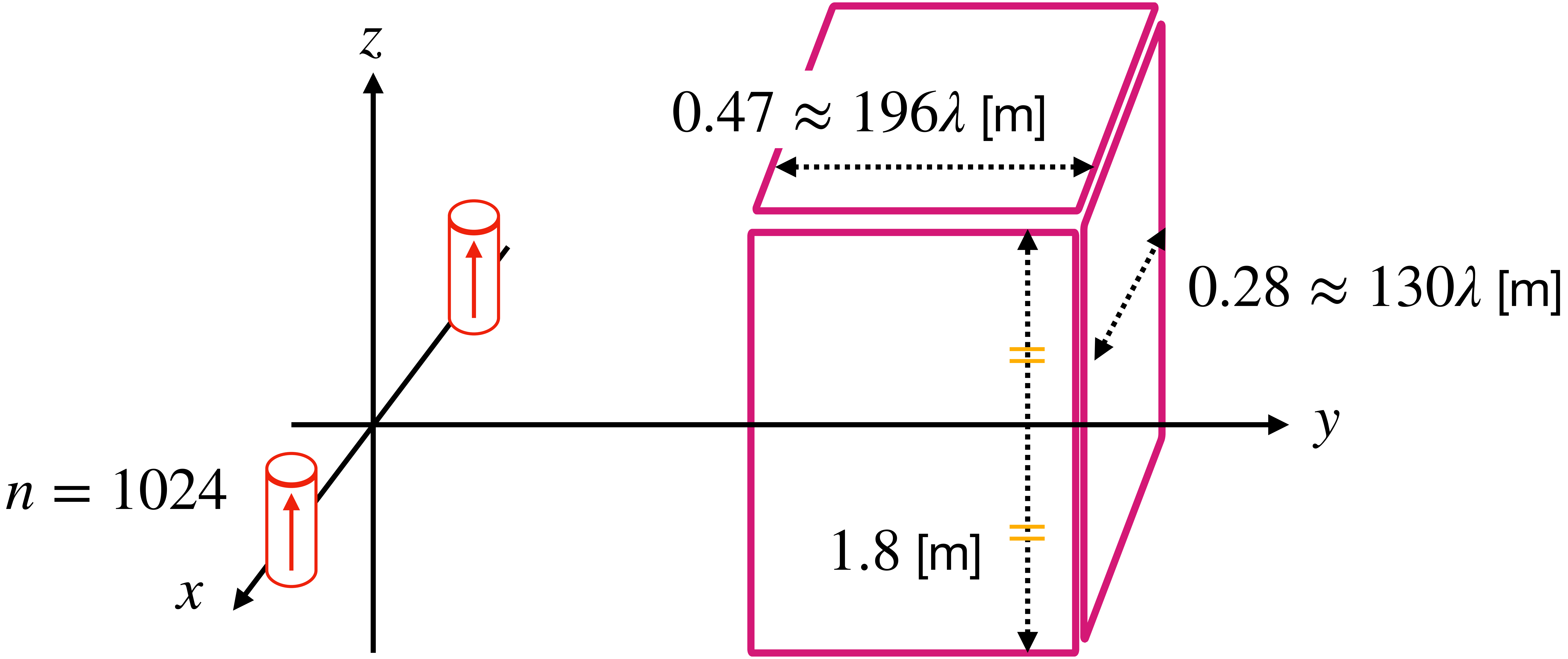

Self-Healing Capability of Bessel Beams

- Consider non-steering cases.
  - The larger α leads to the higher self-healing capability but shorter distance.
  - The smaller α leads to the longer distance but lower self-healing capability.

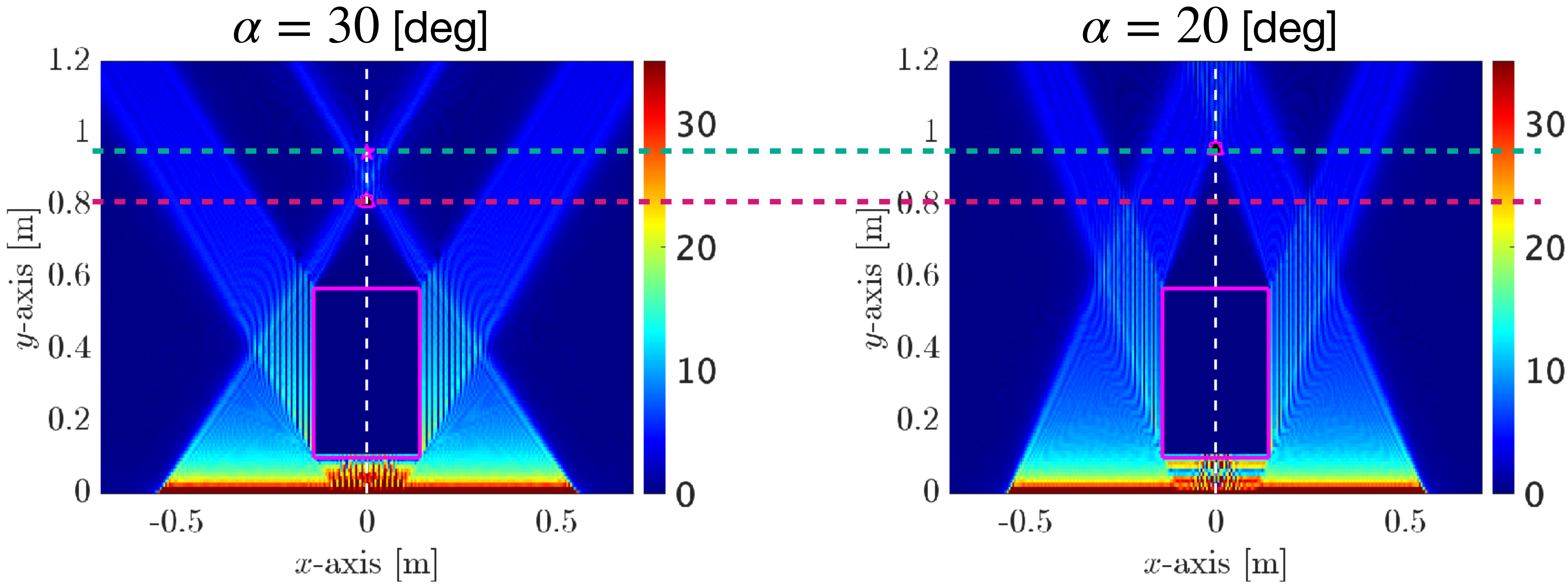

Blockage Avoidance of Curving Beams

- The proposed design achieves the parabolic trajectories based on the user position while avoiding one obstacle.

$(x_u, y_u) = (-0.1, 1)$

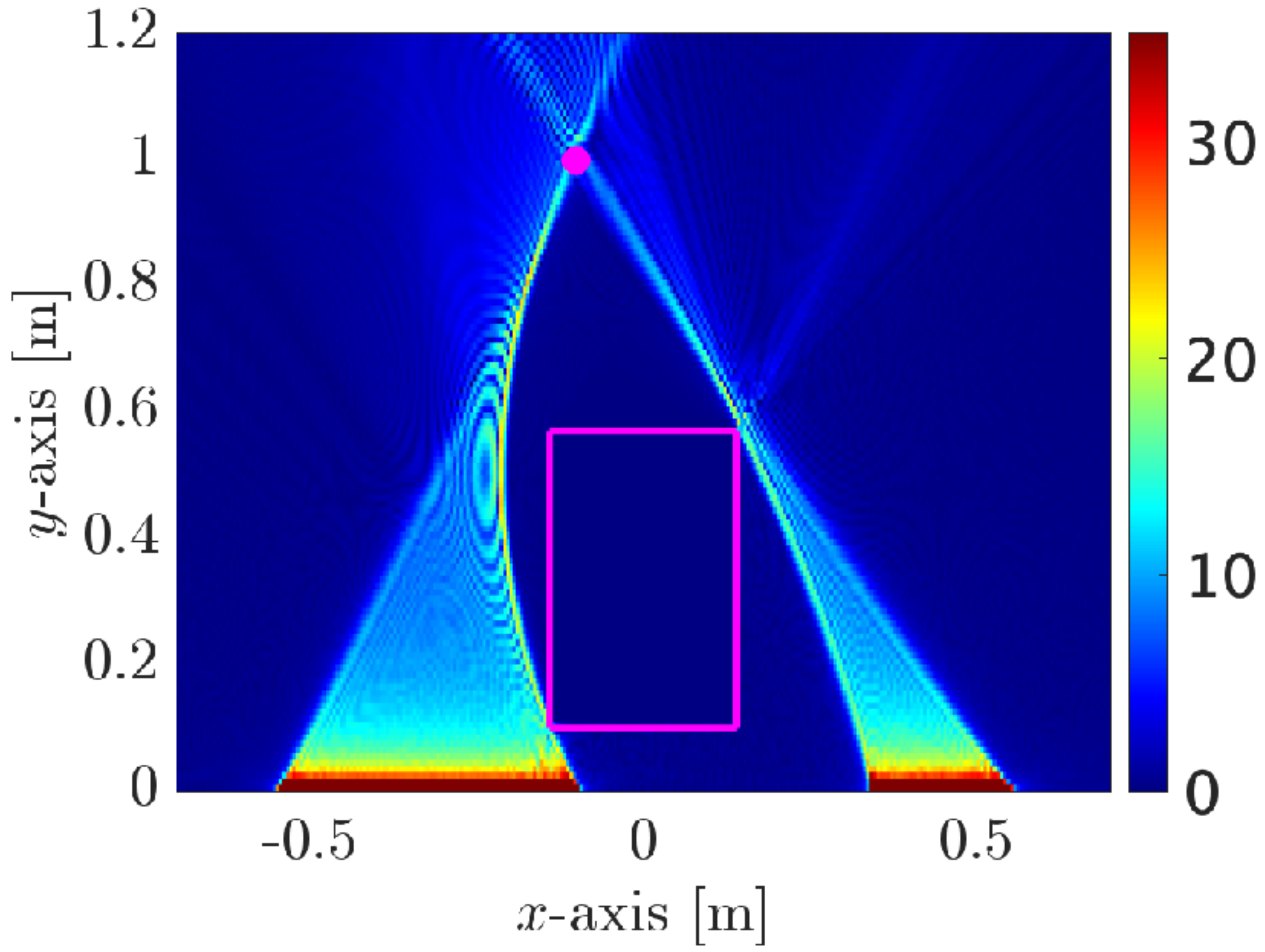

$(x_u, y_u) = (-0.35, 1)$

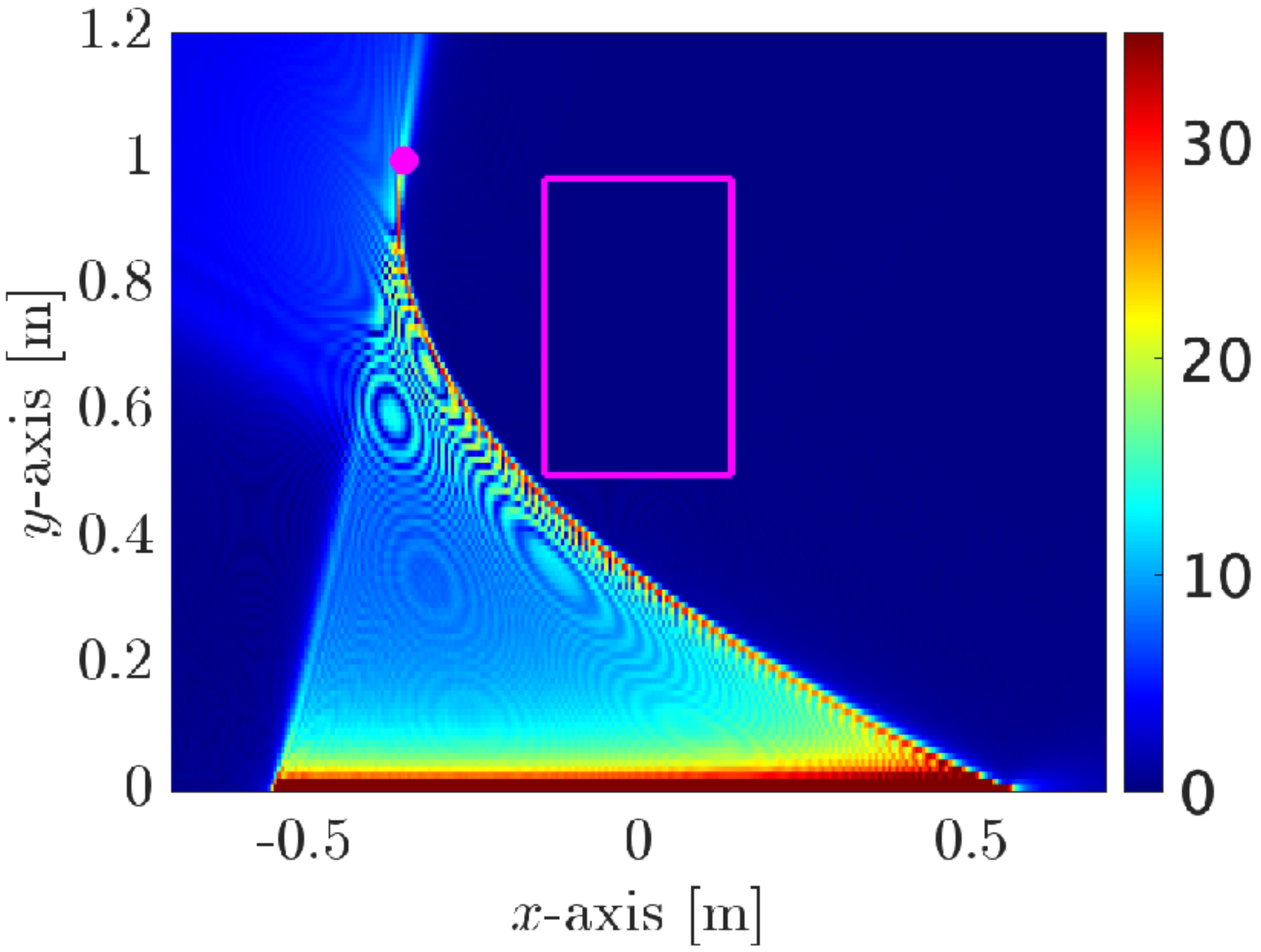

Comparisons With Different Beams

- The phase distribution of the other well-know beams;
  - Gaussian beam: $\phi_n = -k \sin \theta_{\mathrm{A}} x_{\mathrm{t},n}$
  - Beamfocusing: $\phi_n = k r_n$ (r_n is the distance between the user and antenna)

Information used to generate beams with a ULA

	Gaussian beam	Beamfocusing	Bessel beam	Curving beam
User position		✔		✔
Azimuth angle	✔	-	✔	-
Obstacle position			△	✔

Communication Scenario

- The user position is set to $(x_{\mathrm{u}}, y_{\mathrm{u}}) = (0,1)$.
- The potential area of the user in the presence of *positioning errors* is given by $x_{\mathrm{u}} \in [-0.1,0.1]$ and $y_{\mathrm{u}} \in [0.9,1.1]$
- Four points of the obstacle are considered
- Point 0 means no obstacle.

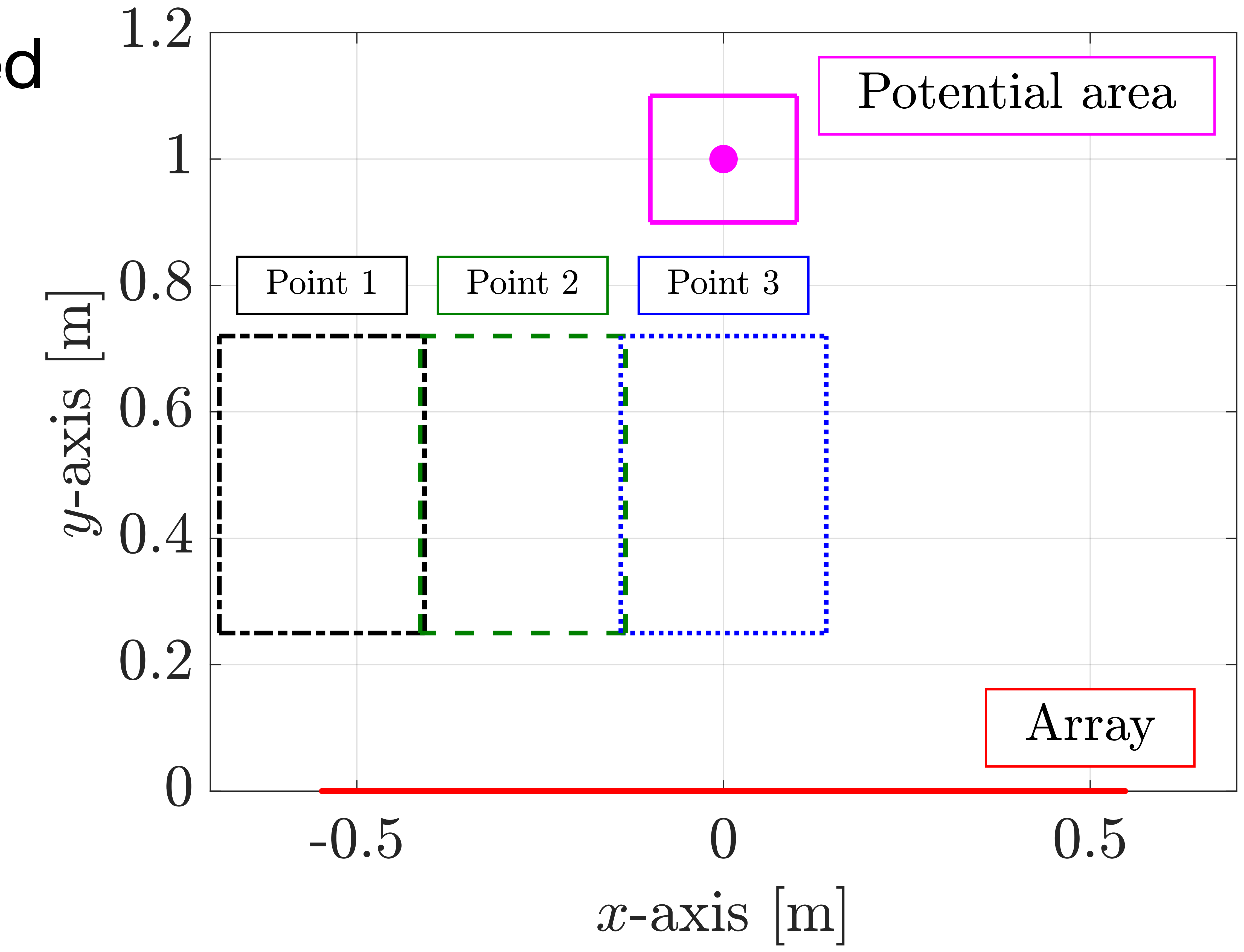

Amplitude of the Electric Field at the User Position

- The beamfocusing achieves the strongest intensity.
- Bessel and curving beams mitigate the blockage effects

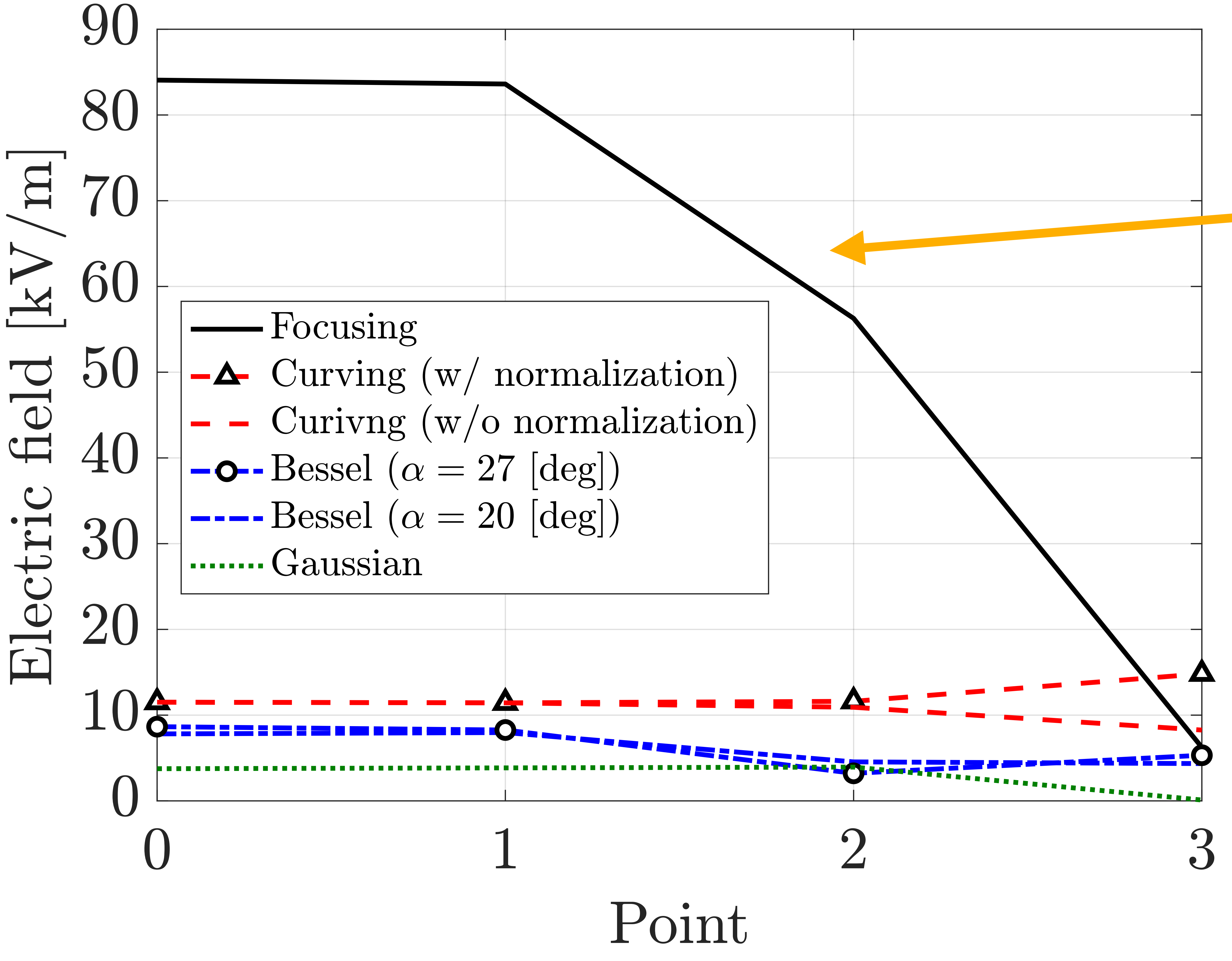

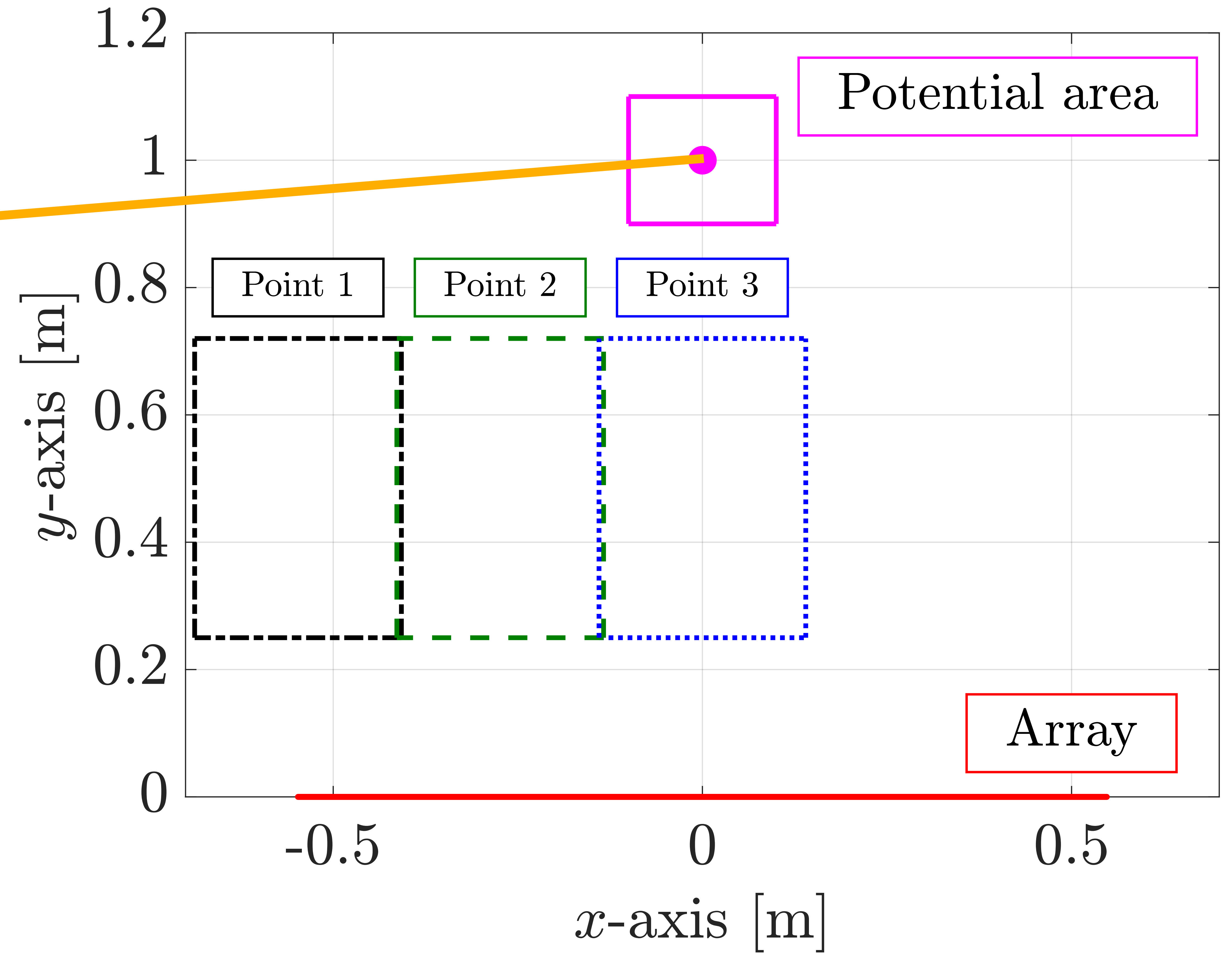

Amplitude of the Electric Field With Positioning Errors

- For beamfocusing, the average intensity is much lower than the maximum one.
- The proper choice of α of Bessel beams depends on the blockage effects.

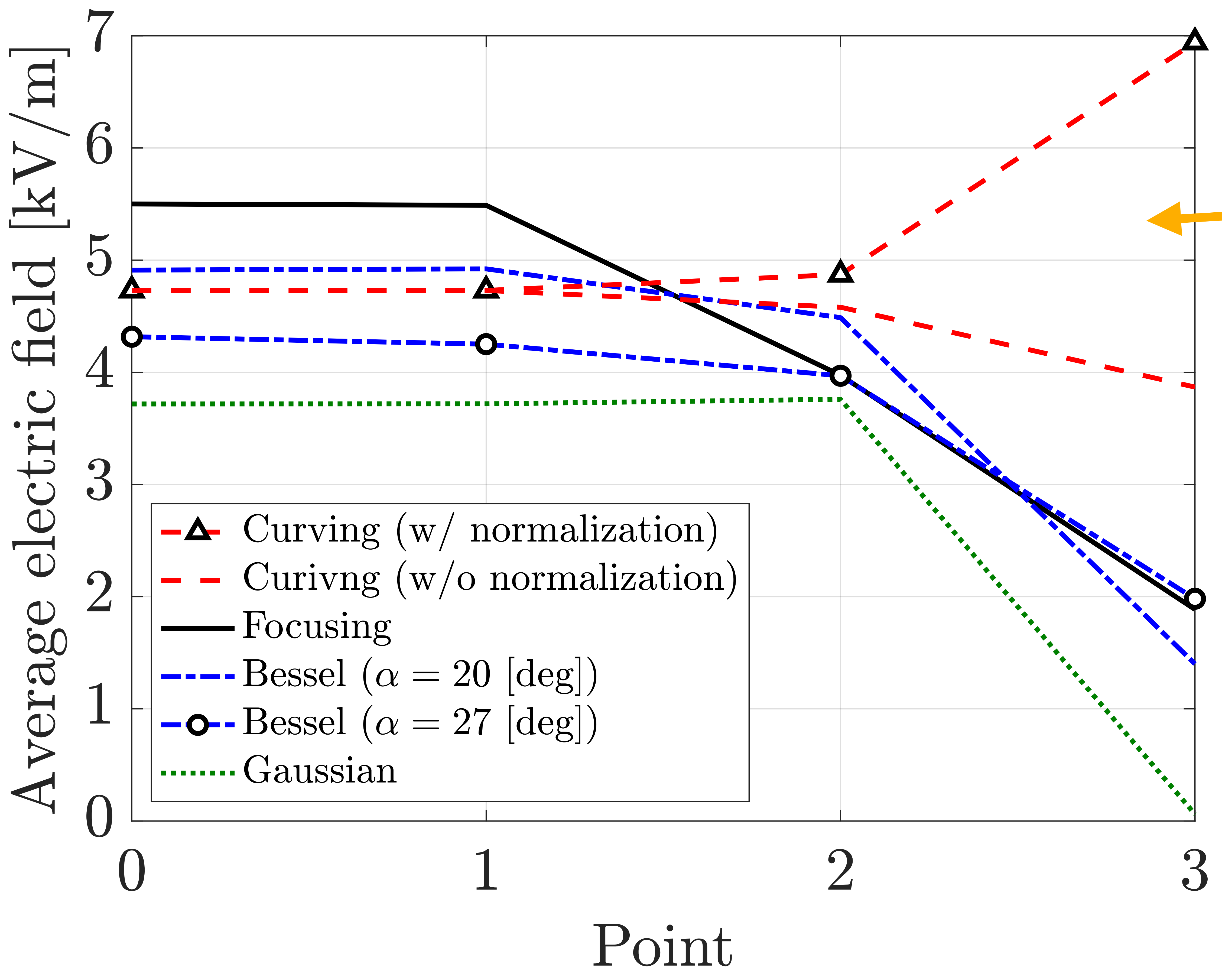

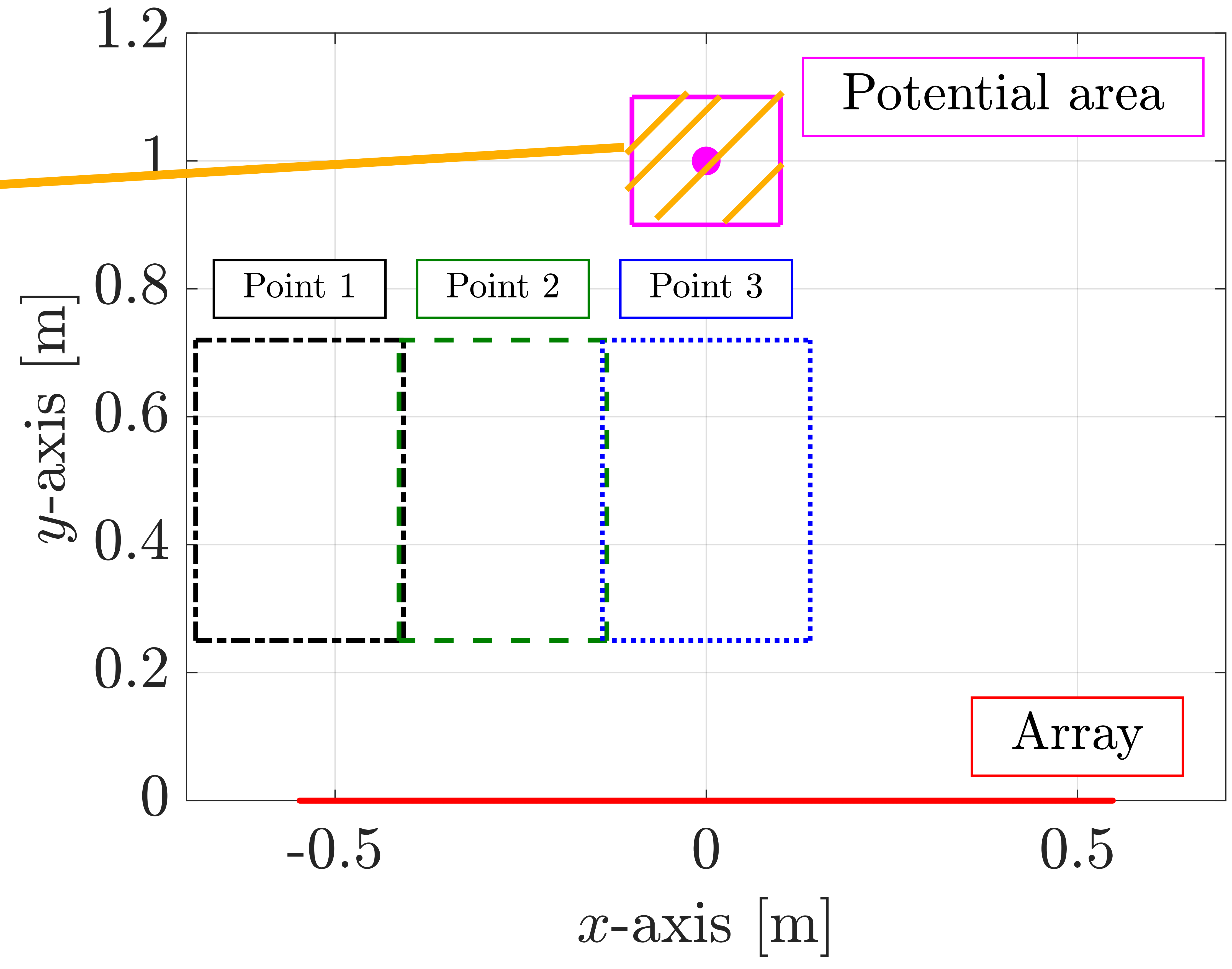

CDF of Amplitude of the Electric Field

- Consider all the situations with positing errors.

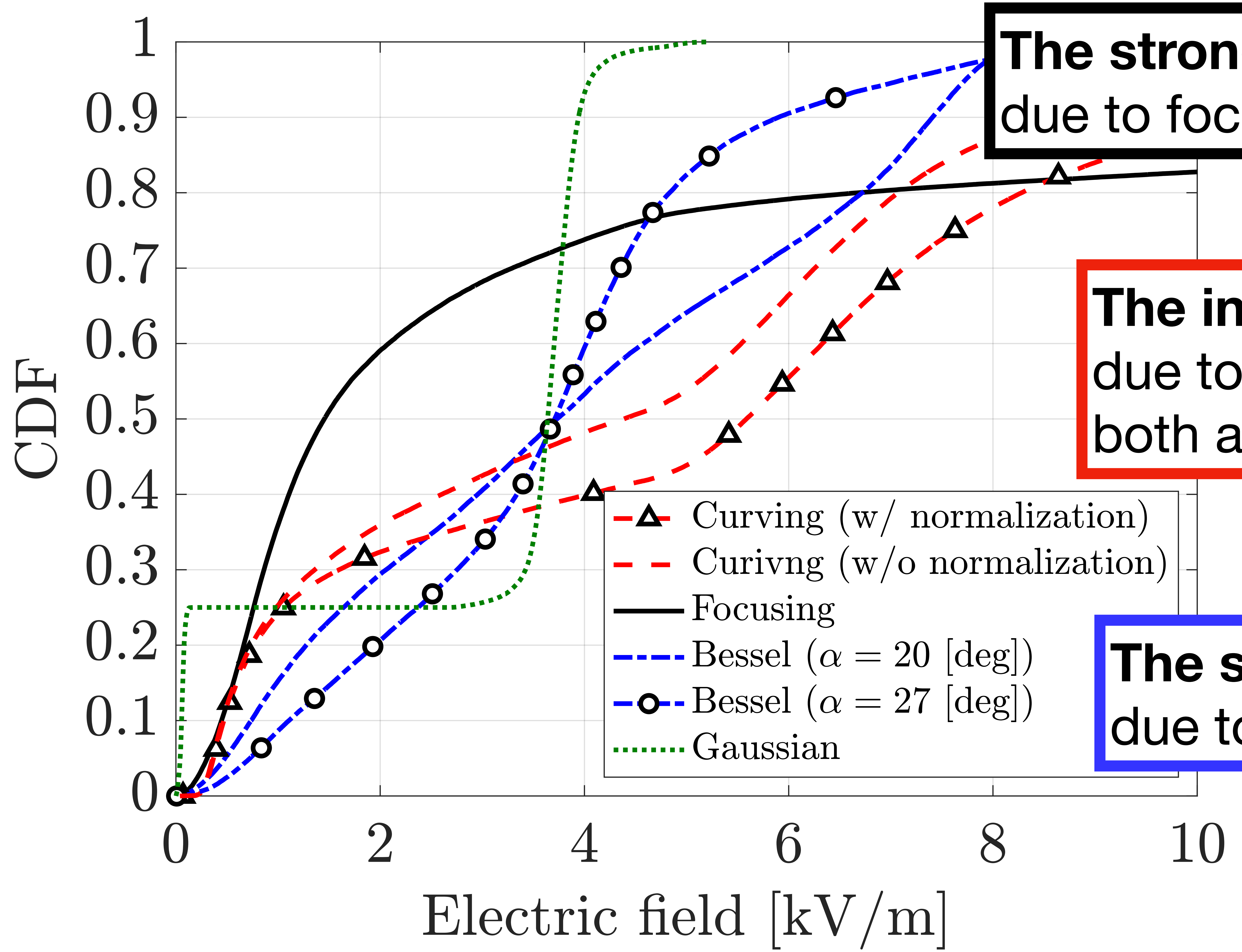

The strongest achievable intensity
due to focal points based on user positions

The intermediate property
due to beam designs with positions of both a user and an obstacle

The strongest minimum intensity
due to beam designs with only angles

CDF of Amplitude of the Electric Field

- Focus on Bessel beams

With the smaller α ($= 20$ [deg]),
the robustness to **position errors** is improved.

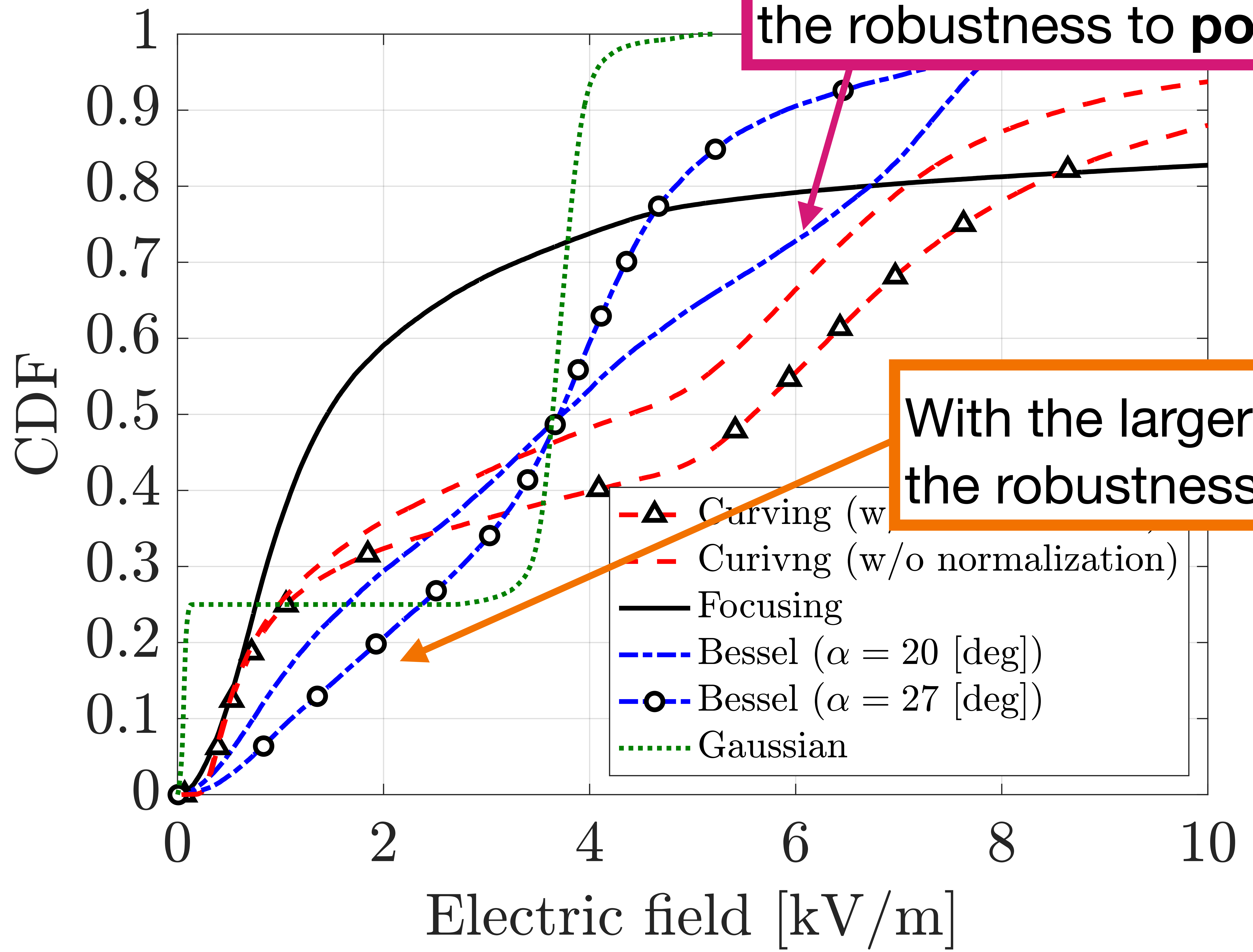

With the larger α ($= 27$ [deg]),
the robustness **against blockages** is improved.

Today's Talk

Advanced Wireless and Communication Research Center

- First part:
  - Near-field beam generation using uniform linear array (ULA)
  - Closed-form phase distributions of near-field beams
  - Properties and conditions of Bessel beam generation

arXiv Paper

- **Second part:**
  - **Full-digital extremely-large (XL-) MIMO systems**
  - **Joint channel and data estimation for multiuser XL-MIMO**

arXiv Paper

Near-Field Channel Estimation for XL-MIMO

- **P-SOMP** [TC'22]
  - Consider near-field channel sparsity using **polar (angle-distance) grids**
  - Assume orthogonal pilot (leads to **large pilot overhead** in XL-MIMO)

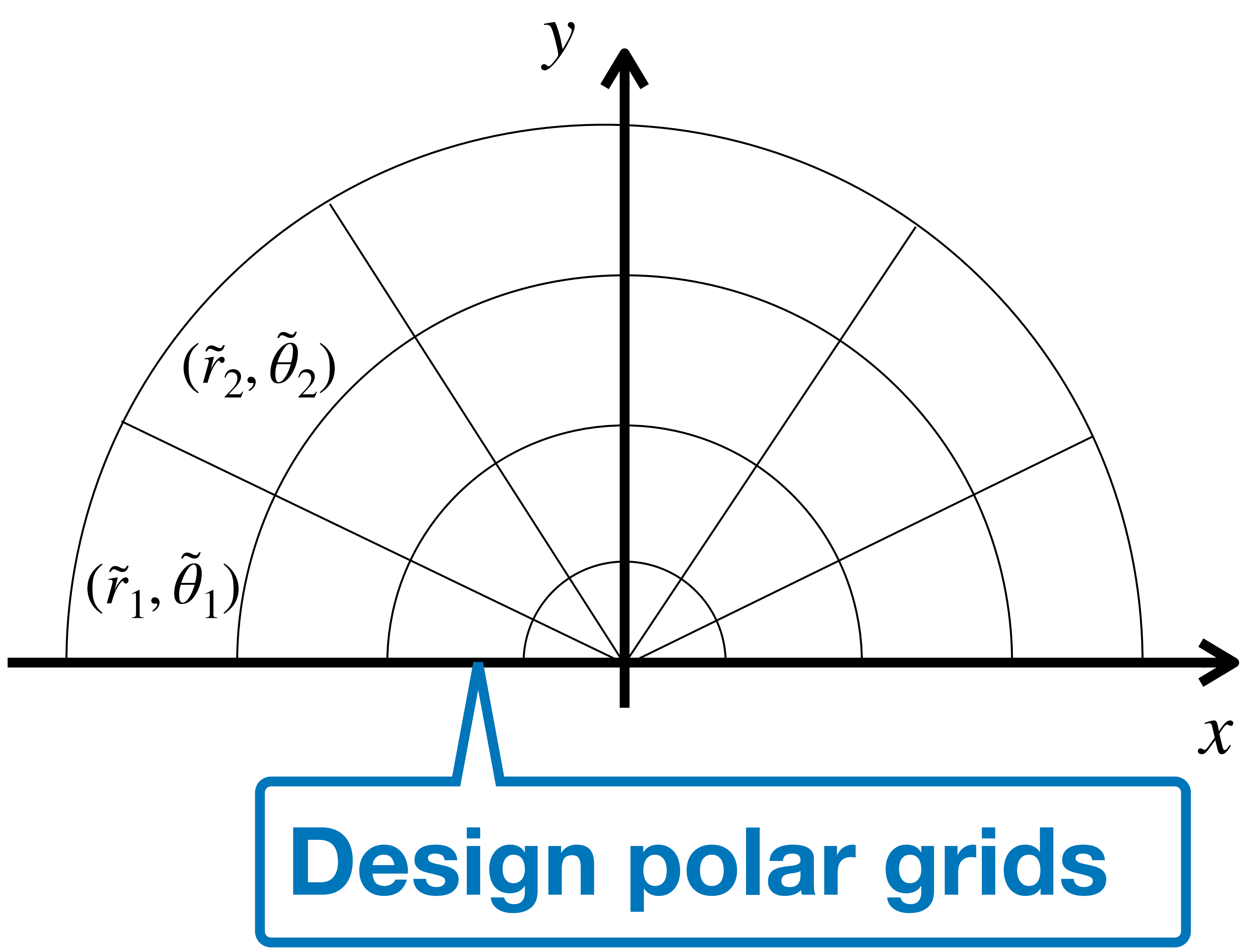

- **2D-CoSaMP** [TC'24], **2-Stage-2D-SOMP** [SP'24]
  - Use non-orthogonal pilots to reduce pilot overhead
  - **Data detection performance is limited** compared to perfect CSI due to non-orthogonality of pilots

[TC'22] M. Cui and L. Dai, IEEE Trans. Commun., 2022.
[SP'24] K. Arai, et.al., in Proc. IEEE SPAWC, 2024.
[TC'24] X. Xie, et.al., IEEE Trans. Commun., 2024.

Purpose and Our Contribution

AWCC Advanced Wireless and Communication Research Center

Purpose of this study

- Accurate data detection and near-field channel estimation for multiuser XL-MIMO systems with small pilot overhead

Contribution

- **JCDE (Joint channel and data estimation) algorithm** based on EP and EM
  - leverages polar sparsity by Bayesian inference with deterministic approach
  - leverages channel correlation by sub-array-wise LMMSE-based filter

EP : Expectation propagation

EM : Expectation maximization

System Model (Uplink Multiuser XL-MIMO)

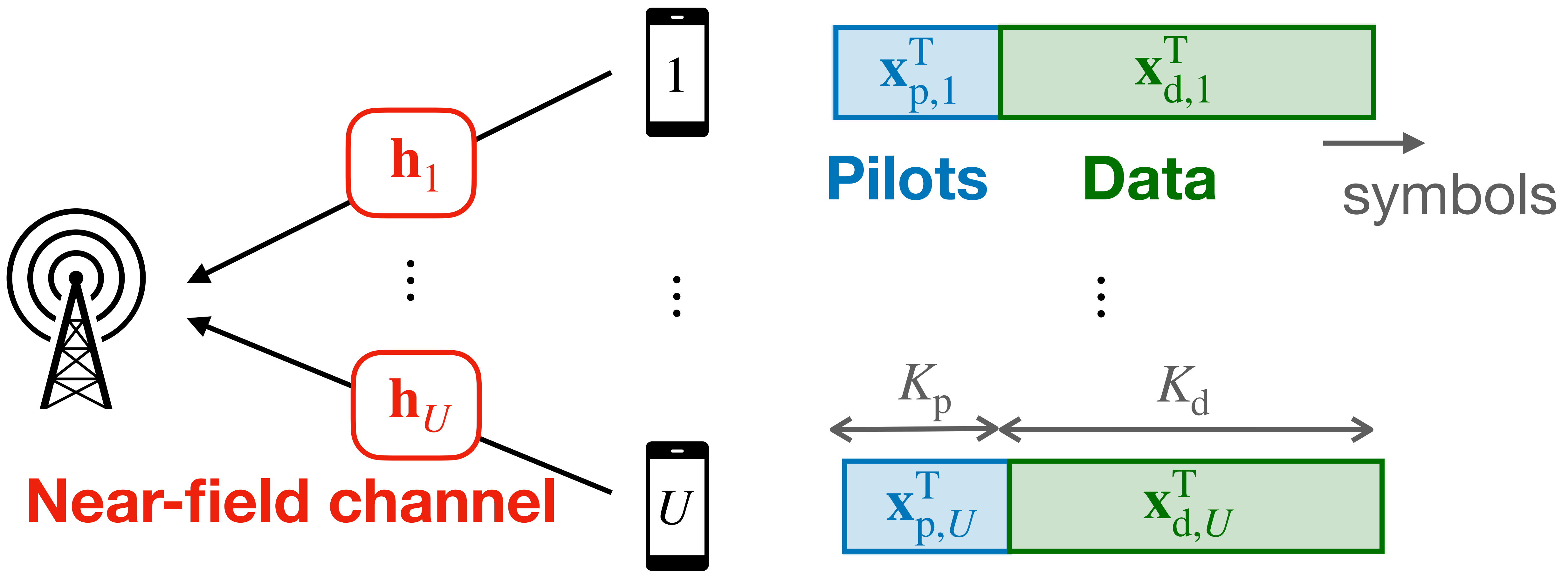

Num. of antennas : N

Num. of UEs : U

Length of pilots : K_{p}

Length of data : K_{d}

Received signal : $\mathbf{Y}$ **Channel :** $\mathbf{H}$ **Tx signals :** $\mathbf{X} = [\mathbf{X}_{\mathrm{p}}, \mathbf{X}_{\mathrm{d}}]$

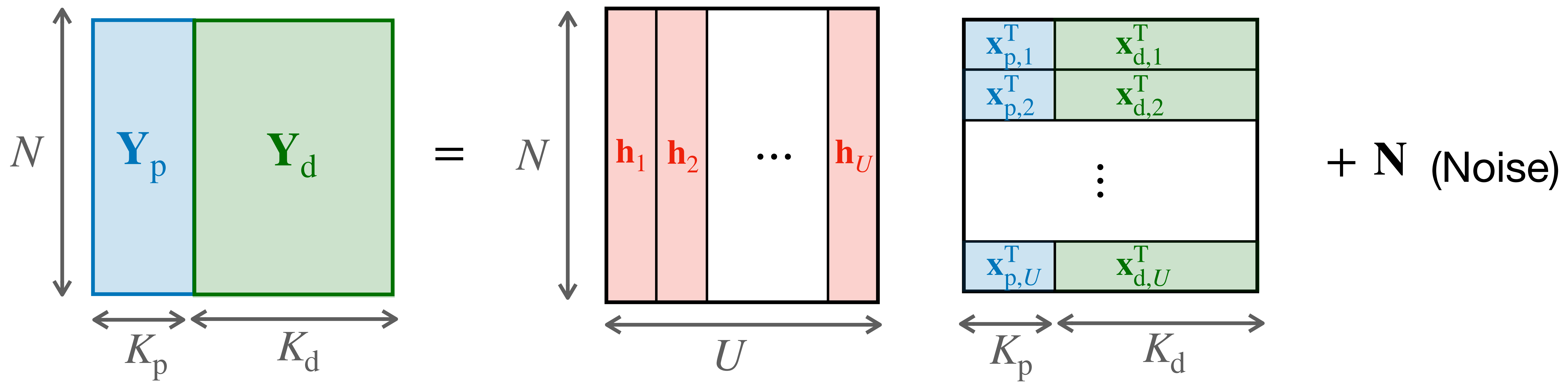

Purpose : Estimate channel $\mathbf{H}$ and data $\mathbf{X}_{\mathrm{d}}$ with pilot $\mathbf{X}_{\mathrm{p}}$

Near-Field Channel Model

- **Near-field channel vector**

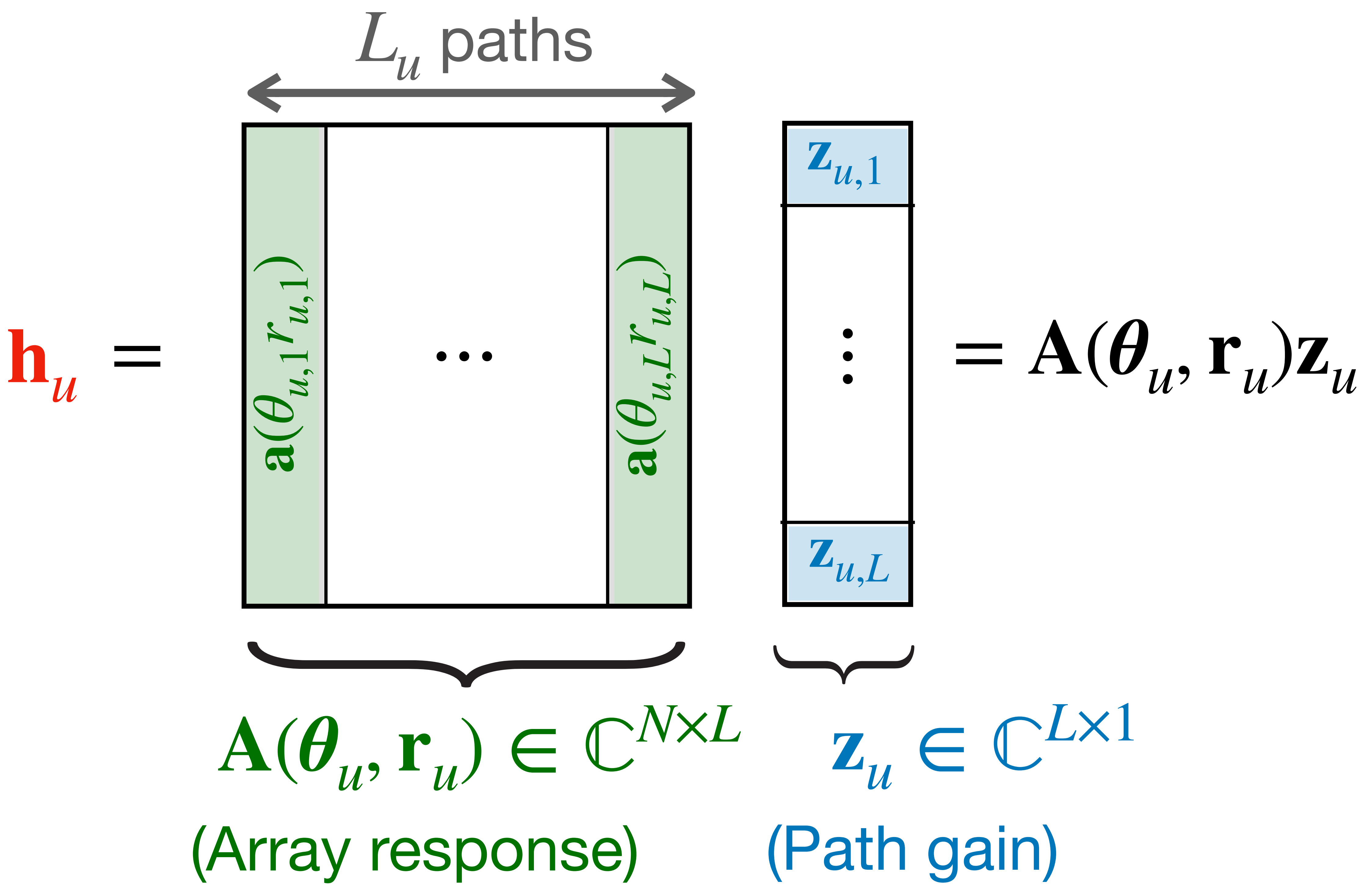

$$[\mathbf{a}(\theta_{u,l}, r_{u,l})]_n = \exp\left[-j\frac{2\pi}{\lambda}\left(r_{u,l}^{(n)} - r_{u,l}\right)\right]$$

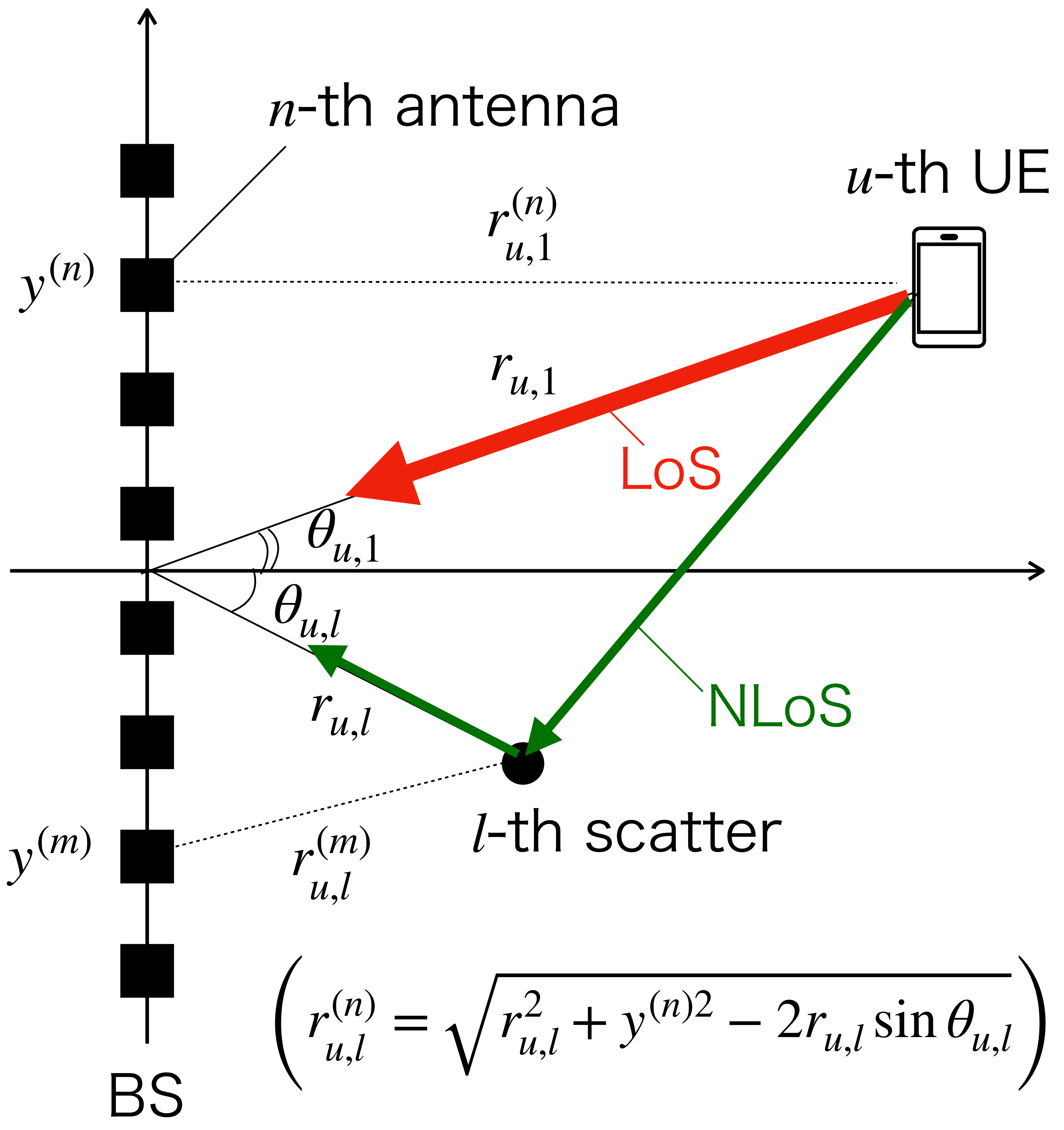

Array response depends on distance r

Near-Field Channel Sparsity

To exploit channel sparsity, transform $\mathbf{H}$ and $\mathbf{Y}$ using DFT matrix $\mathbf{D}_N \in \mathbb{C}^{N\times N}$

$$\mathbf{H} \leftarrow \mathbf{D}_N^{\mathrm{H}}\mathbf{H},\ \ \mathbf{Y} \leftarrow \mathbf{D}_N^{\mathrm{H}}\mathbf{Y}$$

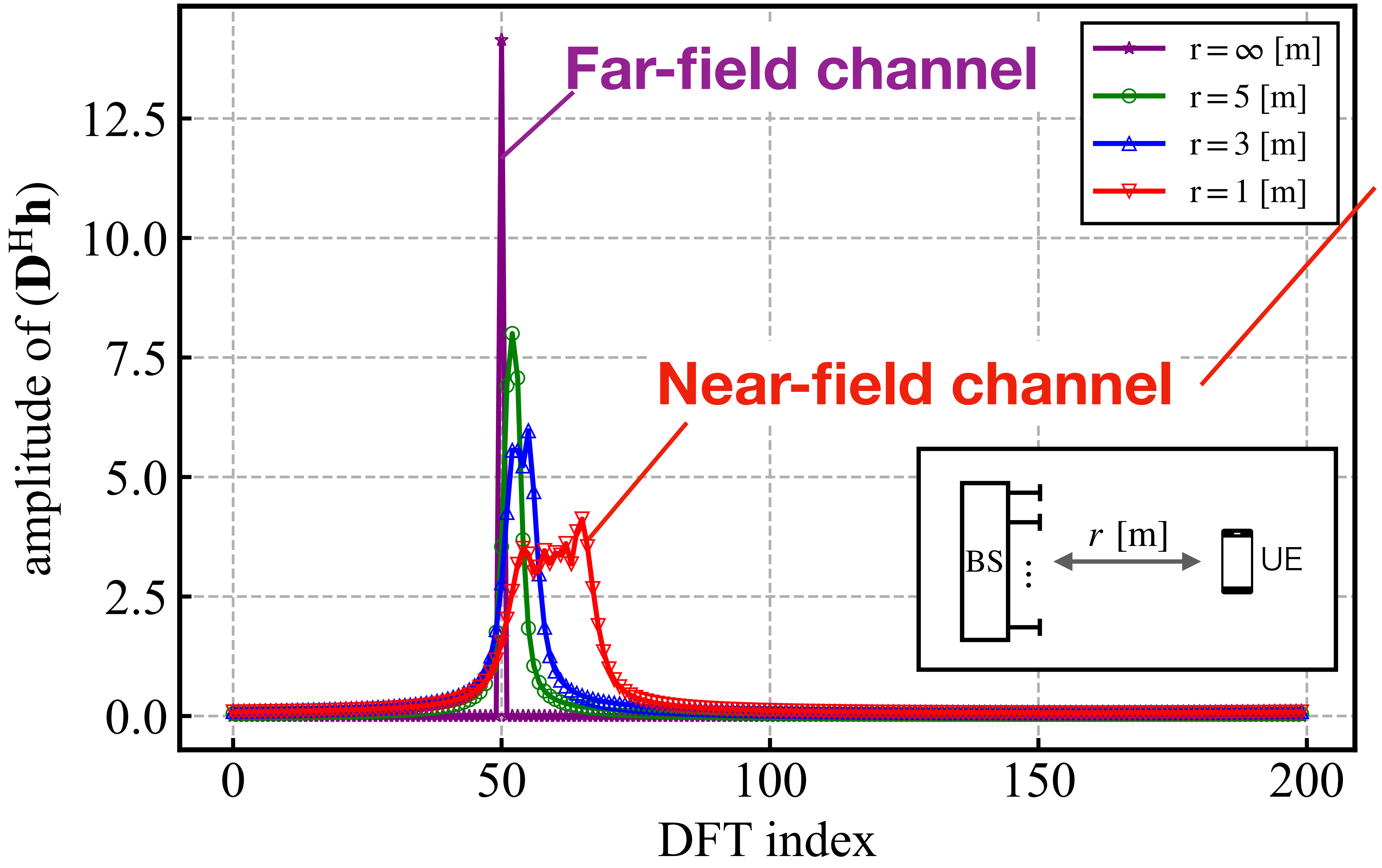

Cluster sparsity due to energy leakage

⇒ Cannot use conventional channel estimation method [JSAC'17] relying on the **far-field assumption**

$N = 200, f_c = 100$ [GHz], antenna aperture 0.3m, Fraunhofer distance 59.4m

[JSAC'17] K. Venugopal, et al., IEEE J. Sel. Areas Commun., 2017.

Model-Based Channel Estimation

To tackle energy leakage effects, decompose $\mathbf{H}$ into $\hat{\mathbf{S}} \in \mathbb{C}^{N\times U}$ and $\mathbf{E} \in \mathbb{C}^{N\times U}$

$$\mathbf{H} = \hat{\mathbf{S}} + \mathbf{E}$$

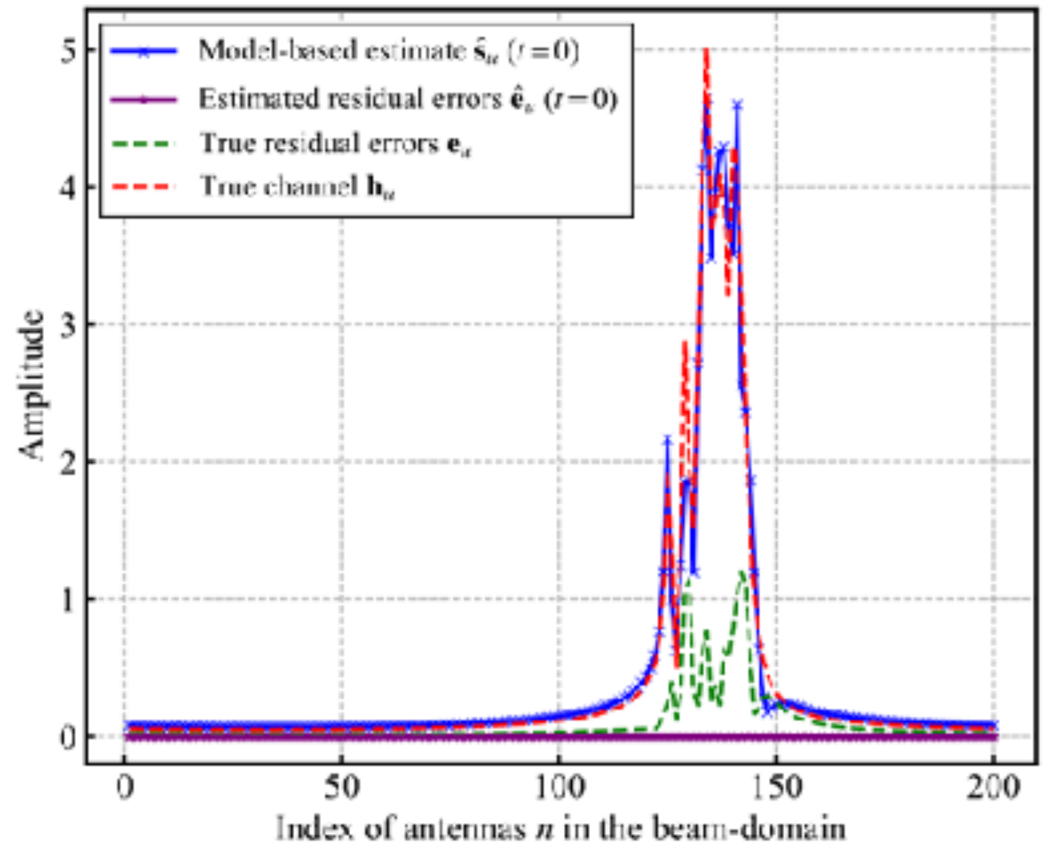

$\mathbf{E}$: Residual error ← As a random variable

$\hat{\mathbf{S}}$: Model-based estimate ← As a deterministic variable

$$\left(\hat{\mathbf{s}}_u = \mathbf{A}(\hat{\boldsymbol{\theta}}_u, \hat{\mathbf{r}}_u)\hat{\mathbf{z}}_u \right)$$

$\mathbf{A}(\hat{\boldsymbol{\theta}}_u, \hat{\mathbf{r}}_u)$: estimated array response

$\hat{\mathbf{z}}_u$: estimated path gain

Estimate

- $\mathbf{E}$ by **Bayesian Inference** with a sparse prior
- $\hat{\mathbf{S}}$ by a **deterministic** approach exploiting near-field structures

Update Model-Based Estimate $\hat{\mathbf{S}}$

- **Sparse reconstruction relying on the near-field structures**

$$\underset{\tilde{\mathbf{z}}_u}{\text{minimize}} \quad \left\| \hat{\mathbf{h}}_u - \hat{\mathbf{s}}_u \right\|_2^2$$

$\hat{\mathbf{h}}_u$: Tentative estimate using $\mathbf{E}$ and the previous $\hat{\mathbf{S}}$

$\hat{\mathbf{s}}_u$: Model-based estimate

$$\text{subject to} \quad \hat{\mathbf{s}}_u = \mathbf{A}(\tilde{\boldsymbol{\theta}}, \tilde{\mathbf{r}})\tilde{\mathbf{z}}_u$$

$$\left\| \tilde{\mathbf{z}}_u \right\|_0 = \hat{L}_u$$

(• $\tilde{\boldsymbol{\theta}} \in \mathbb{R}^{G_\theta \times 1}$: candidate AoAs
• $\tilde{\mathbf{r}} \in \mathbb{R}^{G_r \times 1}$: candidate distances)

Virtual array approximation

$\mathbf{h}_u \simeq$

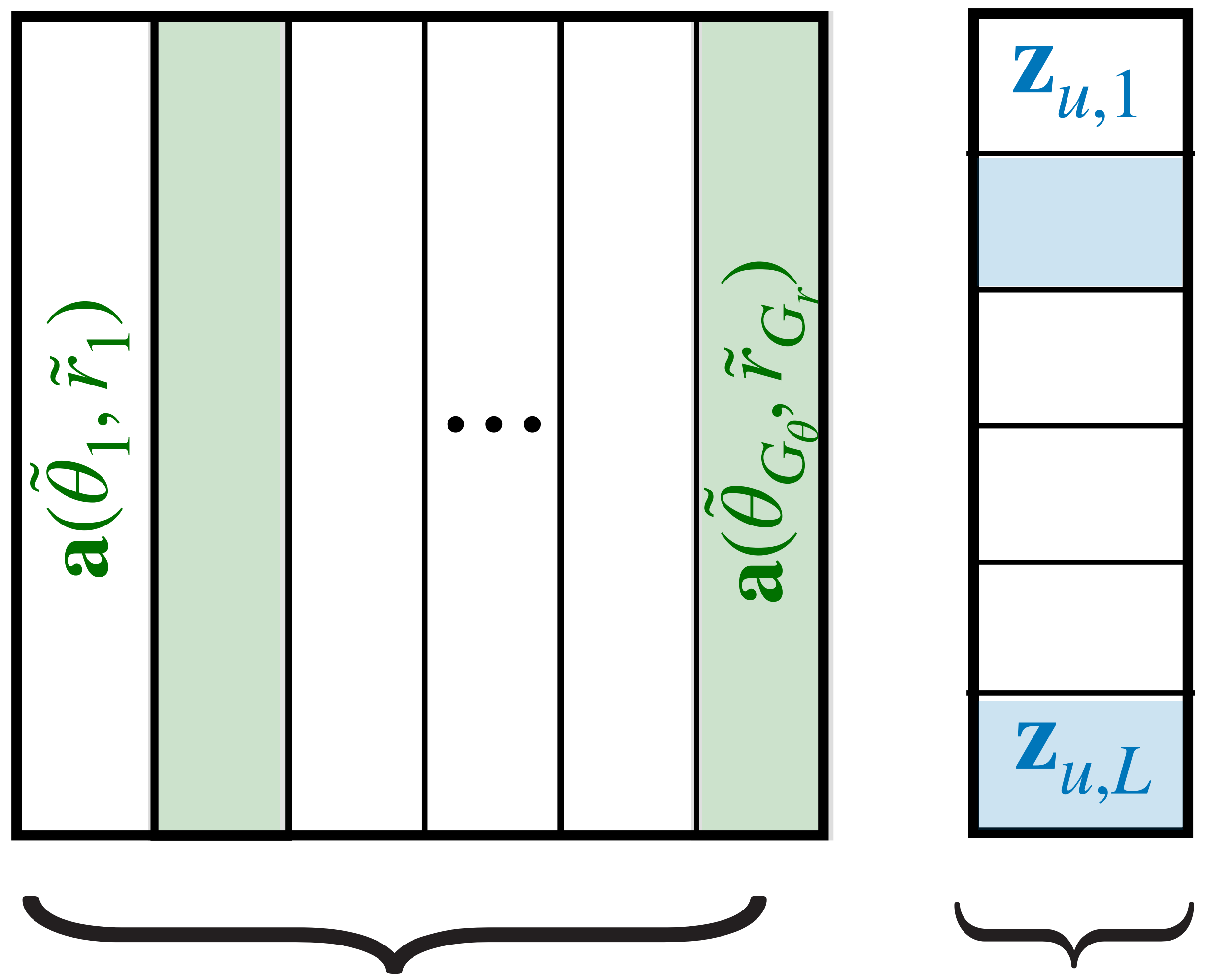

$\mathbf{A}(\tilde{\boldsymbol{\theta}}, \tilde{\mathbf{r}}) \in \mathbb{C}^{N \times G_\theta G_r}$ (Array response)

$\tilde{\mathbf{z}}_u \in \mathbb{C}^{G_\theta G_r \times 1}$ (Path gain)

Proposed JCDE Algorithm

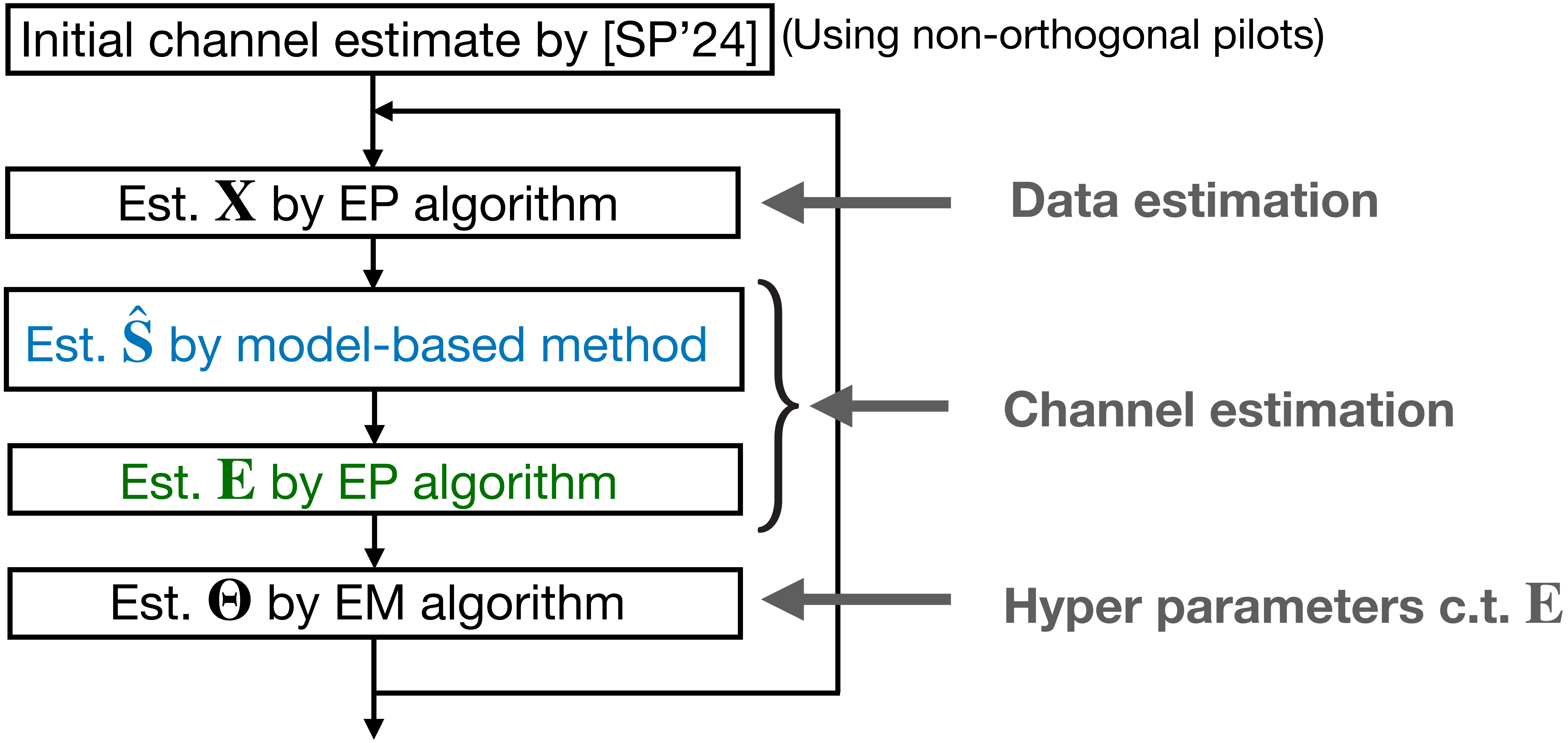

Alternately estimate data and channel in iterations

[SP'24] K. Arai, et.al., in Proc. IEEE SPAWC, 2024.

Performance Assessment: Setup

AWCC Advanced Wireless and Communication Research Center

System parameters

- $N = 200$ (Num. of antennas)
- $U = 50$ (Num. of UEs)
- $K_{\rm p} = 25$ (Num. of pilots)
  - SIDCO frame [VTC’18] (50×25)
- $K_{\rm d} = 100$ (Num. of data)
- $Q = 64$ (64QAM)
- $C = 4$ (Num. of sub-arrays)

Channel parameters

- $L_u = 3$ (Num. of paths per UE)
- $\mathrm{K} = 10$ dB (K-factor)
- $\theta_l \sim \mathcal{U}(-60^\circ, 60^\circ)$ (Angle of arrival)
- $r_l \sim \mathcal{U}(1, 10)$ m (Distance)
- $G_\theta = 395,\ G_r = 7$ (Num. of grids)
- $f_c = 100$ GHz
- antenna aperture 0.3 m
- Fraunhofer distance 59.4 m

[VTC’18] R.-A. Stoica, et.al., in IEEE VTC-Fall, 2018.

NMSE vs. SNR

- $N = 200$, $U = 50$, $K_\mathrm{p} = 25$, $K_\mathrm{d} = 100$, $Q = 64$, $C = 4$

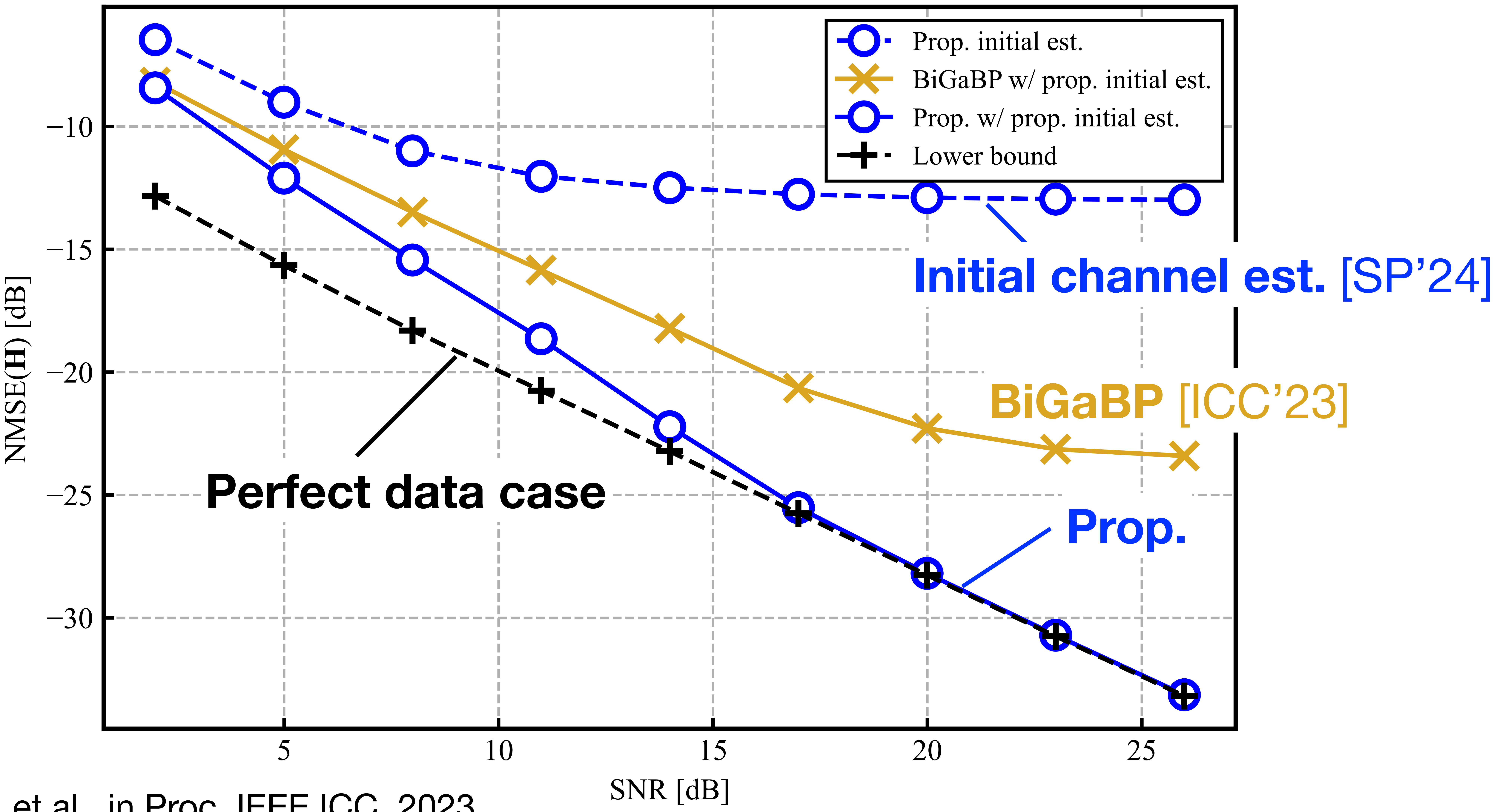

[ICC'23] K. Ito, et.al., in Proc. IEEE ICC, 2023.

BER vs. SNR

- $N = 200$, $U = 50$, $K_\mathrm{p} = 25$, $K_\mathrm{d} = 100$, $Q = 64$, $C = 4$

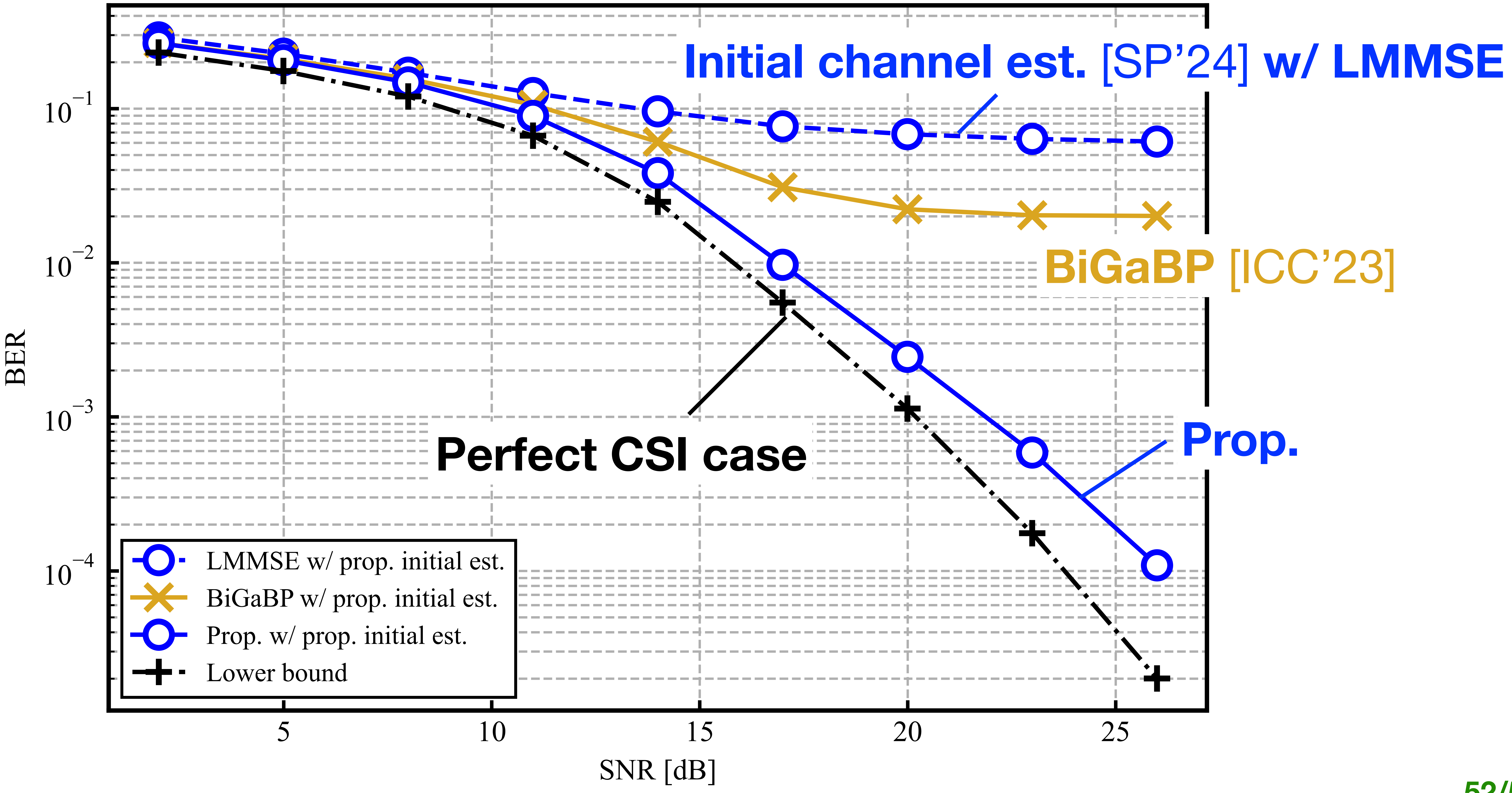

Conclusions and Takeaways

- In this talk
  - Near-field beam generation using uniform linear array (ULA)
  - Joint channel and data estimation for multiuser XL-MIMO
- Beam with full CSI vs Beam with partial CSI
  - Obtaining full CSI is computationally demanding
  - Practical limitation to RF chains and focusing gain [WCL’24]
    - *Focal point blurs* even at 10m despite a 1 km Rayleigh distance
  - Possibility of new design for near-field communications

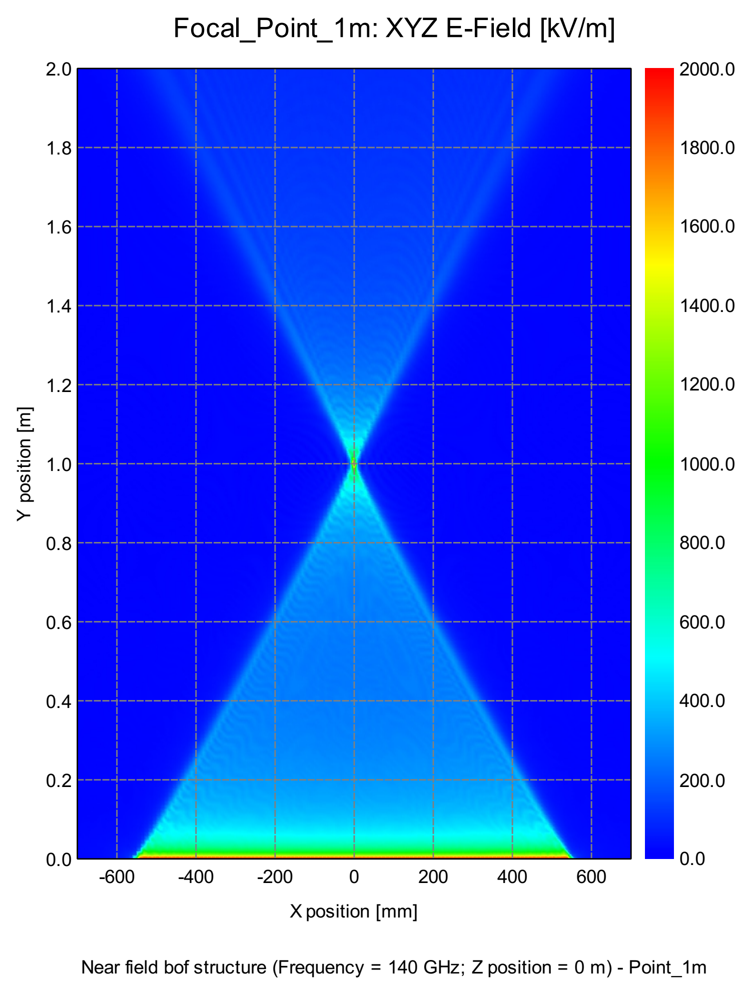

1m

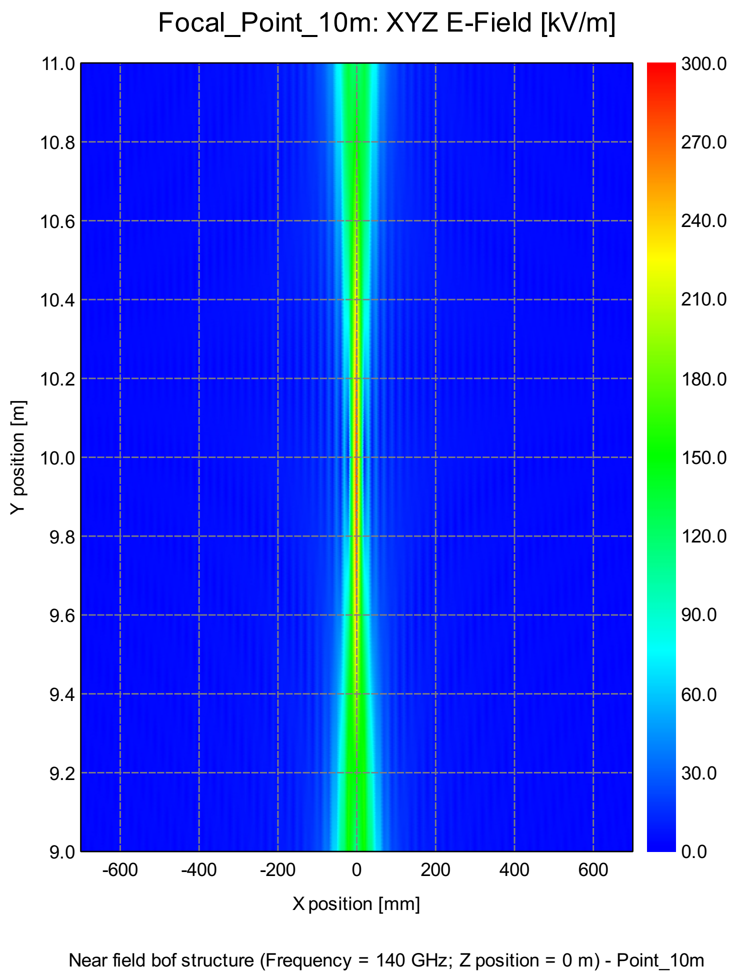

10m

[WCL’24] A. Sakhnini, M. Wachowiak, A. Bourdoux and S. Pollin, "An Approximation of the Range Resolution in the Near-Field of a Distributed Antenna Array," *IEEE Wireless Commun. Lett.*, vol. 13, no. 12, pp. 3281-3284, Dec. 2024,